STANDARD-COMPLIANT AND SOFTWARE DEFINED VLC SYSTEM: IMPLEMENTATION AND PERFORMANCE EVALUATION

A Thesis

by

Waqas Hussain

Submitted to the
Graduate School of Science and Engineering
In Partial Fulfillment of the Requirements for
The Degree of

Master of Science

in the
Department of Electrical and Electronics Engineering

Özyeğin University
August 2015

Copyright © 2015 by Waqas Hussain

STANDARD-COMPLIANT AND SOFTWARE DEFINED VLC SYSTEM: IMPLEMENTATION AND PERFORMANCE EVALUATION

Approved by:

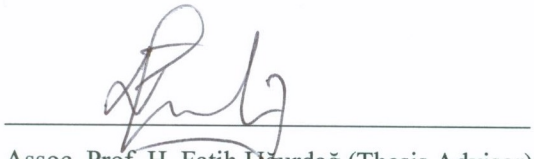

Assoc. Prof. H. Fatih Uğurdağ (Thesis Advisor)

Department of Electrical and Electronics Engineering

Özyeğin University

Prof. Murat Uysal (Thesis Co-Advisor)

Department of Electrical and Electronics Engineering

Özyeğin University

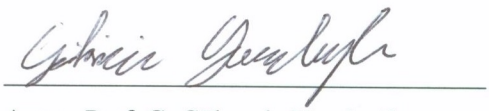

Assoc. Prof. G. Göksenin Yaralıoğlu

Department of Electrical and Electronics Engineering

Özyeğin University

Asst. Prof. Cenk Demiroğlu

Department of Electrical and Electronics Engineering

Özyeğin University

Asst. Prof. Tunçer Baykaş

School of Engineering and Natural Sciences

İstanbul Medipol University

Date Approved: 12th August 2015

This report is dedicated to my teachers, my parents, and my sister.

ABSTRACT

LED lighting is now a cost-effective and energy-efficient technology for general-purpose illumination. Recent advances in LED lighting allow us to use LEDs not only for illumination but at the same time for wireless communication over short distances through a technology called Visible Light Communications (VLC). VLC has been standardized through IEEE 802.15.7 standard. This thesis is the only work in the literature that implements all 9 operating modes of IEEE 802.15.7 PHY I using a Software Defined Radio (SDR) approach in a working real-time prototype with actual LED and photodetector. Our implementation is based on the widely used SDR platform "Universal Software Radio Peripheral" (USRP) and the visual programming software/language LabVIEW. The equipments used in the experimental setup are commercial off-the-shelf devices. We have successfully demonstrated audio streaming through our VLC system, which can transmit and receive data successfully up to 266 kbps at 2 meters. The thesis also includes an extensive set of performance results.

ÖZETÇE

LED ışıklandırma, artık genel amaçlı aydınlatma için uygun maliyetli ve enerji verimli bir teknoloji haline gelmiştir. LED aydınlatmadaki son gelişmeler, bize LED'lerin sadece aydınlatma için değil, aynı zamanda kısa mesafelerde Görünür Işık İletimi (VLC) teknolojisi üzerinden kablosuz haberleşme için de kullanılmasına imkan tanımaktadır. VLC, IEEE 802.15.7 standardı ile standartlaştırılmıştır. Bu tez, literatürde IEEE 802.15.7 PHY'ın 9 çalışma modunun tümünü gerçekleştirmiş tek çalışmadır. Bunun için gerçek LED ve foto detektör ile yaptığımız gerçekzamanlı prototip çalışmasında Yazılım Tabanlı Radyo (SDR) yaklaşımını kullandık. Bizim uygulamamız, yaygın olarak kullanılan SDR platformu "Evrensel Yazılım Radyo Çevresi" (USRP) ve görsel programlama yazılımı/dili LabVIEW tabanlıdır. Deney düzeneğinde kullanılan ekipmanlar, piyasada kolaylıkla bulunabilen cihazlardır. VLC sistemimiz üzerinden 2 metreden 266 kbps'e kadar hızlarda gerçek-zamanlı ses aktarımı başarılı bir şekilde gösterildi. Tez aynı zamanda kapsamlı performans sonuçları da içermektedir.

ACKNOWLEDGEMENTS

First and foremost, I am thankful to Allah Almighty for each and everything. I am particularly thankful to my thesis advisor Assoc. Prof. H. Fatih Uğurdağ who took prodigious interest throughout MS studies. He gave me a lot of motivation as well as encouragement and guided me with many beneficial tips.

I am also very much grateful to my co-advisor Prof. Murat Uysal for his continuous support, persistence supervision, and valuable advices during this thesis work.

I would also like to express thanks to all my OzU family, especially my lab mates for their continuous help and support during my research and studies.

Last but not least, I would like to express my deepest gratitude to my parents. Thanks for their generous and endless love to me. They are always with me whenever I go through tough situations and provide encouragement and support. This research work would not complete without their support. My deepest appreciation goes to them by dedicating this thesis to them.

TABLE OF CONTENTS

ABSTRACT iv

ÖZETÇE v

ACKNOWLEDGEMENTS vi

LIST OF TABLES x

LIST OF FIGURES xi

I. INTRODUCTION 1

1.1 Visible Light 2

1.2 Visible Light Communications (VLC) 2

1.3 VLC Link Configurations 4

1.4 VLC Applications 5

1.5 VLC Standards 6

1.6 VLC Sources and Detectors 6

1.6.1 Light Sources 7

1.6.2 Photodetectors 8

1.7 Comparison and Contribution to the Literature 9

1.8 Thesis Structure 10

II. DESCRIPTION OF THE IEEE VLC STANDARD 11

2.1 Physical Layer Description 11

2.1.1 General Characteristics 12

2.1.2 Dimming and Flicker Mitigation 13

2.2 Types of Physical Layer 13

2.3 PHY I Specifications 15

2.3.1 Forward Error Correction Codes 15

2.3.2 Interleaving and Puncturing 17

2.3.3 Line Coding 18

2.3.4 Modulation 20

III. DESCRIPTION OF THE PROPOSED SYSTEM IMPLEMENTATION 22

3.1 System Models 22

System Model for PHY I 22

3.2 Experimental Setup 24

3.2.1 Transmitter 24

3.2.2 Receiver 26

IV. EXPERIMENTAL RESULTS 28

Critical calculations for Exp. 1 through 8 28

Data rate calculation 28

DC Voltage Calculation 28

4.1 Exp. #1: Output Vpp and Vdc versus Current (with bias-tee) 28

4.2 Exp. #2: Output Vpp and Vdc versus Frequency (with bias-tee) 31

4.3 Exp. #3: Output Vpp and Vdc versus Input Vpp (with bias-tee) 35

4.4 Exp. #4: Max Distance versus Input Vpp (with bias-tee) 38

4.5 Exp. #5: Max Distance versus Frequency (with bias-tee) 40

4.6 Exp. #6: Output Vpp and Vdc versus Current (without bias-tee) 42

4.7 Exp. #7: Output Vpp and Vdc versus Frequency (without bias-tee) 45

4.8 Exp. #8: Output Vpp and Vdc versus Input Vpp (without bias-tee) 48

4.9 Exp. #9: BER Measurements (without bias-tee) 50

4.10 Exp. #10: BER Measurements (MATLAB Simulation AWGN) 52

4.11 Exp. #11: Audio File Streaming (without bias-tee) 54

4.12 Exp. #12: Live Audio Streaming (without bias-tee) 54

V. CONCLUSIONS AND FUTURE WORK 55

APPENDIX: EQUIPMENT DETAILS 56

REFERENCES 61

LIST OF TABLES

Table 1: Comparison of VLC and RF communication technologies [11] 3

Table 2: Comparison of an LED and LD [14, 15] 7

Table 3: Visible light wavelength band plan 12

Table 4: PHY I operating modes 14

Table 5: Generator Polynomial 16

Table 6: Manchester encoding 18

Table 7: Mapping 4B (input) to 6B (output) 19

Table 8: Definition of data mapping for VPPM mode 21

LIST OF FIGURES

Figure 1: Electromagnetic spectrum 2

Figure 2: Link configurations 4

Figure 3: Puncturing pattern to obtain rate-1/2 code 17

Figure 4: Repetition pattern used to obtain the effective rate-1/4 code 17

Figure 5: Puncturing pattern to obtain rate-2/3 code 18

Figure 6: Basic concept of VPPM 21

Figure 7: Block diagram of PHY I software subsystems: (a) Transmitter (b) Receiver [43] 23

Figure 8: VLC experimental architecture [44] 24

Figure 9: The LabVIEW VI for our PHY I design [44] 25

Figure 10: VLC configurations (a) with bias-tee (b) without bias-tee 26

Figure 11: VLC Experimental Setup 27

Figure 12: Input current 20 mA 29

Figure 13: Input current 200 mA 29

Figure 14: Input current 320 mA 29

Figure 15: Input current 480 mA 30

Figure 16: Graph of peak-to-peak output voltage vs input current 30

Figure 17: Graph of output DC voltage vs input current 31

Figure 18: Input frequency 1 kHz (data rate 5 kbps) 32

Figure 19: Input frequency 10 kHz (data rate 50 kbps) 32

Figure 20: Input frequency 20 kHz (data rate 100 kbps) 32

Figure 21: Input frequency 100 kHz (data rate 500 kbps) 33

Figure 22: Input frequency 200 kHz (data rate 1000 kbps) 33

Figure 23: Input frequency 250 kHz (data rate 1250 kbps) 33

Figure 24: Input frequency 300 kHz (data rate 1500 kbps) 34

Figure 25: Graph of peak-to-peak output voltage vs input data rate (frequency) 34
Figure 26: Graph of output DC voltage vs input data rate (frequency) 35
Figure 27: Input voltage of 1 Vpp 36
Figure 28: Input voltage of 5 Vpp 36
Figure 29: Input voltage of 10 Vpp 36
Figure 30: Input voltage of 20 Vpp 37
Figure 31: Peak-to-peak output voltage vs peak-to-peak input voltage 37
Figure 32: Output DC voltage vs peak-to-peak input voltage 38
Figure 33: 2Vpp_10kHz(50kbps)_50cm 39
Figure 34: 5Vpp_10kHz(50kbps)_62cm 39
Figure 35: 10Vpp_10kHz(50kbps)_110cm 39
Figure 36: Distance vs peak-to-peak input voltage 40
Figure 37: 20Vpp_50kHz(250kbps)_180cm 41
Figure 38: 20Vpp_100kHz(500kbps)_80cm 41
Figure 39: 20Vpp_200kHz(1000kbps)_40cm 42
Figure 40: Distance vs data rate (frequency) 42
Figure 41: Input current 20 mA 43
Figure 42: Input current 100 mA 43
Figure 43: Input current 200 mA 44
Figure 44: Input current 450 mA 44
Figure 45: Peak-to-peak output voltage vs input current 44
Figure 46: Output DC voltage vs input current 45
Figure 47: Input frequency 5 kHz (data rate 25 kbps) 46
Figure 48: Input frequency 50 kHz (data rate 250 kbps) 46
Figure 49: Input frequency 200 kHz (data rate 1000 kbps) 46
Figure 50: Input frequency 300 kHz (data rate 1500 kbps) 47

Figure 51: Peak-to-peak output voltage vs data rate (frequency) 47
Figure 52: Output DC voltage vs data rate (frequency) 47
Figure 53: Input voltage of 1 Vpp 48
Figure 54: Input voltage of 5 Vpp 49
Figure 55: Input voltage of 10 Vpp 49
Figure 56: Graph of peak-to-peak input voltage vs peak-to-peak output voltage 49
Figure 57: Peak-to-peak input voltage vs DC output voltage 50
Figure 58: BER VLC HW results of PHY I.a to PHY I.e 51
Figure 59: BER VLC HW results of PHY I.f to PHY I.i 52
Figure 60: BER AWGN Simulation results of PHY1.a to PHY1.e 53
Figure 61: BER AWGN Simulation results of PHY1.f to PHY1.i 54
Figure 62: Laser diode driver (Current source) 56
Figure 63: Bias Tee circuit model and connections 57
Figure 64: Bias-Tee 57
Figure 65: LED SST-50 57
Figure 66: Photodetector PDA36A-EC 58
Figure 67: USRP 2920 59
Figure 68: Daughter board WBX 50-2200 MHz Rx/Tx 59
Figure 69: LFTX daughter board 59
Figure 70: LFRX daughter board 60

CHAPTER

I. INTRODUCTION

The spread of technology in the recent years stands out as one of the most noteworthy phenomena in the history of technology particularly in the area of wireless communications and mobile computing. Wireless communications have become ubiquitous much more rapidly than anyone could have imagined two decades ago, and it will continue to be a key element of modern society in the likely future. Due to massive widespread use of wireless RF based devices and systems, the term “wireless” is used almost synonymously with radio frequency (RF) technologies nowadays. With the continuously ever growing requirement of high speed wireless communications, the demand for RF spectrum is not fulfilling the demand, and the time has come to seriously consider other feasible options for wireless communications using the upper parts of the electromagnetic spectrum, which are not very common till date.

Utilization of the optical band of the electromagnetic spectrum for wireless communications opens doors of opportunities in areas that are yet largely unexplored. The range of optical frequencies is between 300 GHz to 300 Peta Hertz, which include infrared, visible, and ultraviolet bands. Optical Wireless Communications (OWC) systems can be employed in a variety of communication applications ranging from very short range (in the order of millimeters) optical interconnects within integrated circuits through outdoor inter-building links (in the order of kilometers) to satellite communications (larger than 10,000 kilometers) [1].

Currently, OWC systems mainly operate in IR band due to the availability of transmitter and receiver devices only for fiber-optic communications. However, more recently a large number of academicians and industry people are interested in exploration of the visible band (380 to 780 nm) for various OWC applications. This has been elicited by recent advances in solid state lighting technologies, which have enabled the development of highly efficient Light Emitting Diodes (LEDs) for illumination purposes [2]. With attractive features including but not limited to long life expectancy, high tolerance to

humidity, lower power consumption, and reduced heat dissipation, LEDs will gradually replace both incandescent and fluorescent lights and be the ultimate light source in the coming years [3,4].

1.1 Visible Light

It is the portion of the electromagnetic spectrum that is visible to the human eye. It lies between ultra-violet and infrared waves, having a range of 380 to 780 nm (approx.), which corresponds to a frequency band between 430 to 750 THz (approx.).

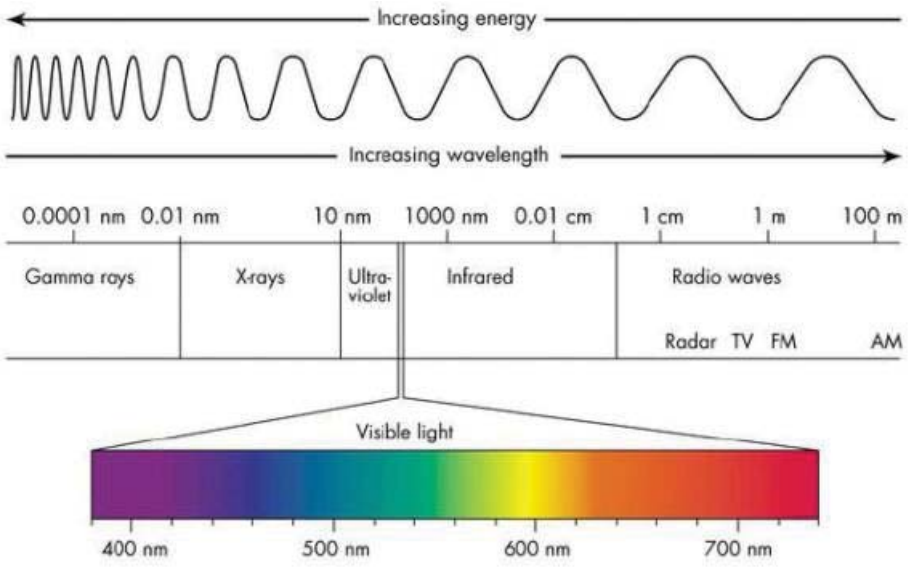

Figure 1: Electromagnetic spectrum

1.2 Visible Light Communications (VLC)

VLC [5] is a new communication technology that uses visible light, particularly LEDs, not only for illumination but also for communication, and is a sustainable and energy efficient approach that has the potential to revolutionize how we use light [6-10]. LEDs can be switched on and off at very high rates, making it possible to transmit data without noticeable effect on lightning output and human eye. VLC, which is also known as Li-Fi, relies on the LED-based illumination infrastructure to enable short-range wireless access. With the expected wide-scale availability of LEDs, VLC is considered as a powerful alternative or complementary to Wi-Fi, a widely used RF technology. VLC offers several other inherent

advantages over traditional RF based counterparts such as immunity to electromagnetic interference, operation in unlicensed bands, additional physical security, and high degree of spatial confinement allowing a high reuse factor. Furthermore, comparison of VLC and RF communication technologies is shown in Table 1.

Table 1: Comparison of VLC and RF communication technologies [11]

Property	**VLC**	**RF**
Bandwidth	Unlimited (380-780 nm)	Regulated and Limited
Electromagnetic Interference	No	Yes
Line of Sight	Yes	No
Distance Range	Short	Short to long (outdoor)
Services	Illumination and communications	Communications
Noise Sources	Sun light and other ambient lights	All electrical/electronic appliances
Power Consumption	Relatively low	Medium
Mobility	Limited	Good
Coverage	Narrow and wide	Mostly wide
Security	Good	Poor

1.3 VLC Link Configurations

The link configurations are categorized on the basis of obstacle existence and the direction between the transmitter and receiver, which are presented below:

- Directed line-of-sight (LOS)
- Non-directed LOS
- Directed non-LOS
- Non-directed non-LOS

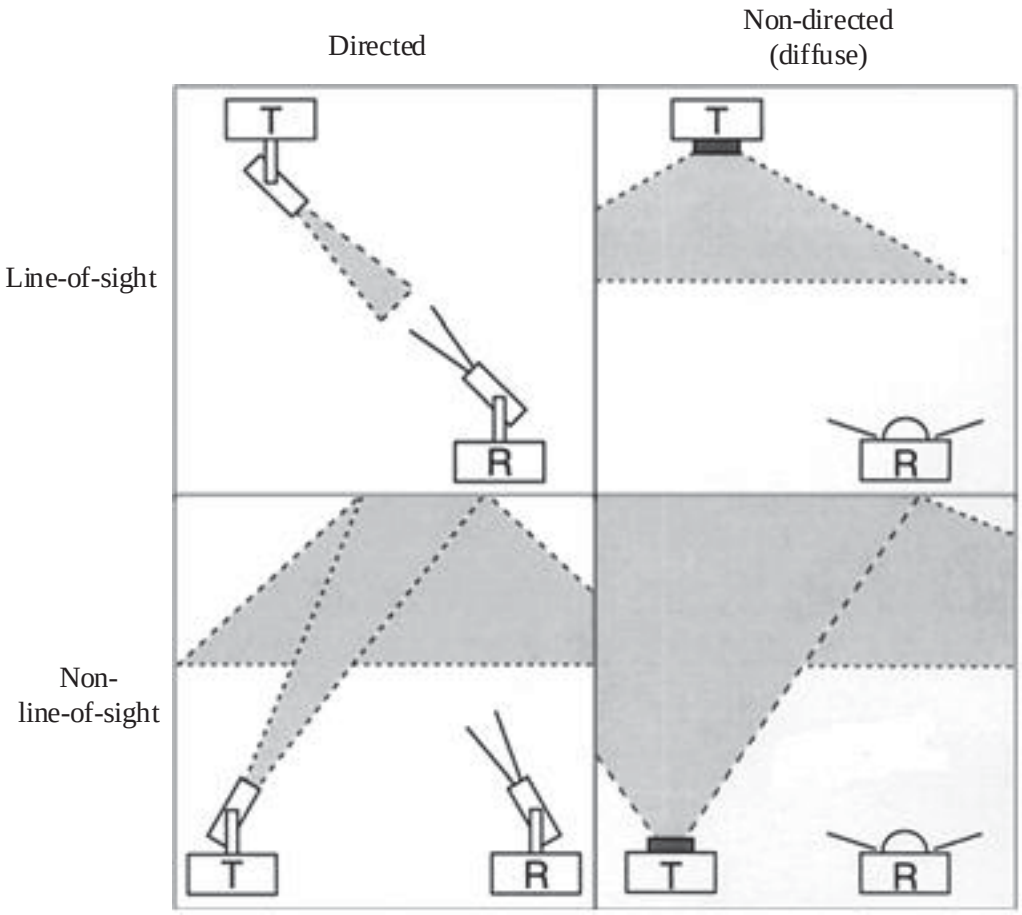

Figure 2: Link configurations

As shown in Figure 2, the directed link design, having transmitters with narrow beam angle and receivers with small field of view (FOV), which maximizes not only the power efficiency but also minimizes path loss and reception of ambient light noise. On the other hand, the non-directed link design,

having transmitters with wide beam angle and receivers with large FOV, alleviates the necessity for pointing accurately as described in the directed link, while at the expenditure of large path loss.

The transmitter in line-of-sight (LOS) link is within the receiver FOV. In non-line-of-sight (NLOS) link, the light source is reflected either from the ceiling, wall or from any other reflecting surfaces. Compared to the LOS link, the path loss of the NLOS link is mostly much superior, while link robustness and ease of use increase, allowing the link to operate even in the presence of obstacles, such as people or objects, between the transmitter and receiver.

In a VLC system, the non-directed LOS link is more generally used due to the indoor illumination environment. From now on, we concentrate only on indoor applications of VLC and non-directed LOS links.

1.4 VLC Applications

It is anticipated that VLC technology based systems and products will be an essential requirement of technology assortment of leading communication companies in the near future. VLC technology can be used for a wide variety of applications and services including but not limited to:

- Smart lightning: VLC provides the infrastructure of smart lightning by controlling illumination and communication through LEDs, and it will greatly reduce energy requirements of a building.
- Mobile connectivity: Content sharing or data transferring between two handheld or portable devices or between a handheld/portable device and a fixed device such as television, computer, printer, etc.
- Hazardous environments: Wireless access in hazardous environments such as petro-chemical plants, mines, etc.
- Vehicle and transportation: Intelligent transportation systems including vehicle-to-vehicle communication (via the use of headlights/taillights) and vehicle-to-infrastructure (e.g., traffic lights) communication.

- Defense and security: Visible light communications is a completely secure technology. Since visible light cannot go beyond walls, so it cannot be detected outside a room.
- Hospitals and healthcare: Wireless access in RF-restricted or prohibited areas such as newborn nurseries, operation theaters, etc.
- Wi-Fi spectrum release: VLC can provide high speed internet in parallel with traditional Wi-Fi, which helps in reducing the Wi-Fi traffic load.
- Aviation: LEDs are already used for illumination in aircrafts and can also be used for providing entertainment services to passengers.
- Underwater communications: As we know that RF does not work well underwater but visible light can work without having any problem and support high speed data transmission over short distances in this environment. Making it possible for divers and underwater vehicles to communicate with each other.
- Location based services: Each LED light is assigned a unique identity that can provide location specific information.

1.5 VLC Standards

Due to the above mentioned wide range of applications of the VLC technology, industrialists and academicians started thinking about standardizing VLC. Japan Electronics and Information Technology Industries Association (JEITA) was the first to release a VLC standard in 2007 [12]. Later on in 2011, the Institute of Electrical and Electronics Engineers (IEEE) published a standard on VLC [13]. The details of the standard published by IEEE are presented later in this report.

1.6 VLC Sources and Detectors

A VLC system can be implemented using several different types of light sources and photodetectors, which are described in the section below.

1.6.1 Light Sources

Light sources that can be used for optical communication must have suitable wavelength, numerical aperture, high radiance with a small emitting surface, long life, high reliability, and high modulation bandwidth. There are mainly two types of light sources used in VLC depending on the requirement and environmental conditions. First one is incoherent light source such as LED, which is used for shorter distance and indoor environment and another one is coherent light source such as laser diode (LD), which is used for longer distance and outdoor environments due to the high profile beam of laser diode.

Comparison of LED and LD

Table 2 gives a succinct comparison between an LED and LD.

Table 2: Comparison of an LED and LD [14, 15]

Characteristics	LED	LD
Optical output power	Low power	High power
Modulation bandwidth	Tens of kHz to hundreds of MHz	Tens of kHz to tens of GHz
Eye safety	Considered eye safe	Must be rendered eye safe
Directionality	Beam is broader and spreading	Beam is directional and is highly collimated
Reliability	High	Moderate
Coherence	Non-coherent	Coherent
Temperature dependence	Little temperature dependence	Very temperature dependent
Cost	Low	Moderate to high
Harmonic distortions	High	Less

LED and its types

LED is a much better light source for VLC compare to LD as shown in Table 2. The LED that is recommended normally for indoor usage is White LED (WLED). There are two types of WLEDs, which are explained below. The performance of these WLEDs is determined by several important parameters. These parameters include color stability, color rendering capability, and luminous efficacy.

Phosphor based WLED

In phosphor based WLEDs, yellow phosphor is added to monochromatic blue LED, much in a similar way a fluorescent light bulb works. The majority of WLEDs that are currently available in the market are manufactured using this technology. Apart from the advantage of requiring only a single color source, these types of WLEDs are easier to design and less expensive. Additionally, in order to achieve a higher modulation bandwidth, and therefore higher data rates, the most appropriate method for these WLEDs is to detect only the blue part of the spectrum at the receiver side, which is known as blue filtering [16].

RGB based WLED

RGB based WLEDs can be formed by adding three different color lights, which include red, green, and blue. These WLEDs are also known as multi-color white LED. RGB based WLEDs are not very widely used because rise in the temperature causes emission power to decay exponentially, resulting in a substantial change in color stability.

1.6.2 Photodetectors

There are four types of photodetectors commonly used in optical communication:

- Positive Intrinsic Negative (PIN) photodiode
- Avalanche Photodiode (APD)
- Photoconductor
- Metal–semiconductor–metal photodetector (MSM photodetector)

The PIN and APD are the most widely used photodetectors in OWC systems.

PIN Photodiode

PIN photodiode consists of heavily doped *p* and *n* regions separated by an intrinsic (*i*) region [17]. When used in reverse biased configuration, it acts like a nearly constant capacitance. PIN photodiodes are proficient in operating at a very high bit rate exceeding 100 Gbps [18-20]. Additionally, due to packaging limitations the commercially available devices only offer bandwidth up to 20 GHz.

Avalanche Photodiode

The avalanche photodiode (APD) is different from PIN diode in a way that it offers higher sensitivity but there is always a multiplicative noise associated with the APD due to the statistical nature of the ionization/avalanche process [21]. The avalanche process is also temperature sensitive. These factors are very important and must always be taken into account whenever an APD is used in an optical communication system.

1.7 Comparison and Contribution to the Literature

In line with the growing attention from academia and industry, there is a rapidly growing literature on VLC, see e.g., [22,23], and references therein. In addition to the theoretical investigations and algorithmic-level designs, several research groups have also reported experimental VLC studies exploring practical implementation aspects of VLC systems [24-33]. Some of these experimental studies [24,25] are based on pure hardware solutions involving the use of integrated circuit boards. Such traditional hardware devices limit cross-functionality and can only be modified through physical intervention. Some other experimental studies [26-30] are based on reconfigurable hardware solutions involving the use of either FPGA boards or DSP boards. Such reconfigurable hardware devices require highly skilled and specialized personnel. In contrast to the above mentioned implementations, software defined platforms [34] provide efficient, relatively easy to implement, and inexpensive solutions, where some or all of the PHY functionalities are implemented through modifiable software or firmware operating on programmable processing technologies. This allows new wireless features and capabilities to be added to existing systems without requiring new hardware.

Software Defined Radio (SDR) is commonly used in the wireless industry for rapid prototyping. Similarly, there have been some sporadic efforts to implement software defined VLC systems [31-33]. In [31], Y. Qiao et.al. implemented two VLC links using OFDM on WARP [35] boards. In [32], M. Rahaim et.al. employ Universal Software Radio Peripheral (USRP), an SDR platform, integrated with a VLC front-end. They use GNU Radio [36] for programming purposes and implement BPSK, QPSK, and OFDM modulation schemes in their experimental setup. In [33], J. Baranda et.al. use a modified version of USRP2 from Ettus Research [37] and adopt FlexiCom [38], which is an object-oriented open source software library. The work in [33] aims to achieve video streaming and uses IEEE 802.15.7 PHY I mode with an overrun clock, where the system clock data rate is set to 500 kHz, 2.5 times faster than the rate stated in the standard in order to cope with the extra signaling of the MPEG stream.

In this thesis work, we adopt a similar approach to [33], where modified USRPs are integrated with a VLC front-end. We, however, use National Instruments LabVIEW software, which has a rich set of built-in PHY functions and is fully compatible with USRPs. This thesis is the only work in the literature that implements all 9 operating modes of IEEE 802.15.7 PHY I using an SDR approach in a working real-time prototype with actual LED and photodetector. The equipments used in the experimental setup are commercial off-the-shelf devices. We have successfully demonstrated audio streaming through our VLC system, which can transmit and receive data successfully up to 266 kbps at 2 meters. The thesis also includes an extensive set of performance results.

1.8 Thesis Structure

The remainder of the thesis report is organized as follows. In Chapter II, details about IEEE 802.15.7 standard and main features of its PHY I is provided. In Chapter III, a standard compliant VLC system is presented with detailed description of hardware and software subsystems. In Chapter IV, performance results of basic hardware equipments and BER results of VLC setup are presented. Finally, in Chapter V we conclude.

CHAPTER

II. DESCRIPTION OF THE IEEE VLC STANDARD

The Institute of Electrical and Electronics Engineers (IEEE) recognized the potential of VLC technology and produced IEEE Standard 802.15.7 [13], which was approved in June 2011. This standard defines a physical layer (PHY) and medium access control (MAC) layer for VLC and promises data rates sufficient to support audio and video multimedia services. The introduction of such global standard that is particularly backed by leading companies is expected to further accelerate the developments in this emerging field. An overview of this standard can be found in tutorial type papers [39,40].

More recently, there is ongoing work to write a revision of IEEE 802.15.7-2011 standard. In addition to visible light, now it includes (1) Optical Camera Communication, (2) LED-ID, and (3) Li-Fi.

In this chapter, firstly general description of all three PHY layers of IEEE 802.15.7 standard is provided. Later on, detailed description of PHY I of the aforementioned standard is provided.

2.1 Physical Layer Description

The Physical Layer defines the electrical, physical, and procedural interface between devices and transmission medium. One device transmits data over the medium, while another device receives data from that medium based on the physical layer properties. The functions and services of the physical layer are link establishment and termination of a connection to a communication medium. The implementation of this layer is often known as PHY layer. Based on the IEEE 802.15.7 standard for VLC, PHY layer is responsible for the following tasks [13]:

- Activation and deactivation of the VLC transceiver
- Wavelength Quality Indication (WQI) for received frames
- Channel selection
- Data transmission and reception

- Error correction
- Synchronization

2.1.1 General Characteristics

Operating Wavelength Range and Band Plan for VLC

According to the aforementioned standard the spectrum of the visible light covers wavelengths between 380 nm and 780 nm. The device compliant with standard shall operate in one or several of the following visible light wavelength bands as summarized in Table 3 [13].

Table 3: Visible light wavelength band plan

Wavelength range (nm)	**Center (nm)**	**Spectral width (nm)**	**Code**
380-478	429	98	000
478-540	509	62	001
540-588	564	48	010
588-633	611	45	011
633-679	656	46	100
679-726	703	47	101
726-780	753	54	110
Reserved			111

The information provided in the above table may be used by the receiver for optimizing its performance. The standard also supports use of wide bandwidth optical transmitters (such as white LEDs).

Maximum Error Tolerance for Multiple Optical Sources

If communication protocol is implemented using multiple optical sources, then it is recommended that all optical sources must have similar frequency response in order to assist communication. Furthermore, digital input must be synchronized to all optical sources from the PHY.

WQI Support for OOK and VPPM

The quality of a received signal can be determined by WQI measurement. The WQI measurement may be implemented using either an estimation of signal-to-noise ratio or either by detecting the energy of the received signal, or a combination of both of these methods.

2.1.2 Dimming and Flicker Mitigation

The two main challenges for communication using visible light spectrum are dimming and flicker mitigation.

Dimming

Dimming is defined as controlling the amount of the perceived brightness of the light source according to the user desire. Dimming is one of the important requirements of the VLC system. It helps in saving power and making the system energy efficient. It is required to maintain communication while a user arbitrarily dims the light source.

Flicker Mitigation

The fluctuation in the brightness of light is known as flicker. It can cause noticeable effect on humans especially in terms of physiological effects. The IEEE standard endeavors for the mitigation of flicker that may be caused due to modulation of the light sources used for communication. In order to avoid flicker, change in the brightness time period must not be longer than maximum flickering time period (MFTP). The MFTP is defined as the maximum time period over which the light intensity can be changing, but without being noticed by human eye [41].

There are two types of flicker in VLC according to its generation mechanism: intra-frame flicker and inter-frame flicker. The perceivable brightness fluctuation within a frame termed as intra-frame flicker and between adjacent frame transmissions is termed as inter-frame flicker.

2.2 Types of Physical Layer

IEEE 802.15.7 describes a standard for short range VLC utilizing the unregulated visible light spectrum between from 380 nm to 780 nm [13]. The standard supports three PHY types, namely, PHY I, PHY II,

and PHY III. PHY I uses on-off keying (OOK) and variable pulse position modulation (VPPM). It supports concatenated coding with Reed-Solomon (RS) and Convolutional Coding (CC). This PHY type is intended for outdoor usage with low data rate applications and supports data rates of 11.7 kbps to 266.6 kbps. Similar to PHY I, PHY II uses OOK and VPPM but at higher optical clock rates, aiming to achieve data rates in the tens of Mbps. It supports only RS coding. This PHY type is intended for indoor usage with moderate data rate applications and supports data rates between 1.25 and 96 Mbps. PHY I and PHY II also support a Run Length Limited (RLL) code to provide DC balance, clock recovery, and flicker mitigation. PHY III is intended for applications with multiple light sources and detectors. It uses color shift keying (CSK) and RS coding. This type targets to achieve data rates of 12 to 96 Mbps. In this report, we are focusing on the implementation of PHY I.

Table 4: PHY I operating modes

PHY I Mode	**Data Rate**	**Modulation**	**RLL code**	**Optical clock rate**	**FEC**	
					Outer code (RS)	**Inner code (CC)**
a	11.67 kbps	OOK	Manchester	200 kHz	(15,7)	1/4
b	24.44 kbps				(15,11)	1/3
c	48.89 kbps				(15,11)	2/3
d	73.3 kbps				(15,11)	None
e	100 kbps				None	None
f	35.56 kbps	VPPM	4B6B	400 kHz	(15,2)	None
g	71.11 kbps				(15,4)	None
h	124.4 kbps				(15,7)	None
i	266.6 kbps				None	None

2.3 PHY I Specifications

As mentioned earlier, PHY I is intended for outdoor usage with low data rate applications and supports data rates of 11.7 kbps to 266.6 kbps as shown in Table 4.

2.3.1 Forward Error Correction Codes

Physical layer I of IEEE 802.15.7 standard supports various forward error correcting (FEC) techniques used for removing errors and controlling errors which occur during data transmission. These coding techniques are:

- Reed-Solomon error correcting codes
- Convolutional code

Due to the fact that PHY I is used for outdoor applications, stronger codes using concatenated Reed-Solomon (RS) and convolutional codes (CC) have developed to overcome the problems of additional path loss due to longer distance and potential interference introduced by noise sources such as daylight and fluorescent lighting. RS and CC are preferred over other coding schemes due to their ability to interface well with run length limited (RLL) line codes [40].

Reed-Solomon Codes

In coding theory, RS codes are non-binary cyclic error-correcting codes, which deliver a systematic technique of code generation that could not only detect but also correct multiple random symbol errors. In RS coding, source symbols are considered as coefficients of a polynomial over a finite field known as Galois Field (GF).

In the case of PHY I systematic RS codes are used with GF (2^4), generated by the '$x^4 + x + 1$' polynomial. The generators for the RS (n, k) codes for PHY I are given in Table 5, where α is a primitive element in GF (2^4) [13].

Table 5: Generator Polynomial

(n, k)	g(x)
(15, 11)	$x^4+\alpha^{13}x^3+\alpha^6x^2+\alpha^3x+\alpha^{10}$
(15, 7)	$x^8+\alpha^{14}x^7+\alpha^2x^6+\alpha^4x^5+\alpha^2x^4+\alpha^{13}x^3+\alpha^5x^2+\alpha^{11}x^1+\alpha^6$
(15, 4)	$x^{11}+\alpha^9x^{10}+\alpha^8x^9+\alpha^4x^8+\alpha^9x^7+\alpha^{13}x^6+\alpha^4x^5+\alpha^{12}x^4+\alpha^4x^3+\alpha^5x^2+\alpha^3x+\alpha^6$
(15, 2)	$x^{13}+\alpha^3x^{12}+\alpha^8x^{11}+\alpha^9x^{10}+\alpha^2x^9+\alpha^4x^8+\alpha^{14}x^7+\alpha^6x^6+\alpha^{10}x^5+\alpha^7x^4+\alpha^{13}x^3+\alpha^{11}x^2+\alpha^5x+\alpha$

If the last block does not meet the block size requirements, then it is recommended to use shortened Reed-Solomon code. In order to minimize padding overhead, shortened RS code is used for frame sizes not matching code word boundaries [13].

Starting with a RS (n, k) code, one can get an RS (n-s, k-s) shortened code as follows:

- Pad the k-s RS symbols with s zero RS symbols.
- Encode using RS (n, k) encoder.
- Delete the padded zeros (do not transmit them).
- At the decoder, add the zeros, then decode.

Convolutional Codes

It is a based on a rate-1/3 mother convolutional code having constraint length seven (K=7) with generator polynomial $g_0 = 133_8$; $g_1 = 171_8$; $g_2 = 165_8$. In order to terminate the convolutional code, six tail bits of zeros shall be added at the end of it.

Rate-1/4 Code

The rate-1/4 code is obtained by puncturing the rate-1/3 mother code to a rate-1/2 code, as shown in Figure 3, and then using a simple repetition code as shown in Figure 4.

Rate-1/3 Code

The rate-1/3 code is obtained by using the outputs of the rate-1/3 mother code.

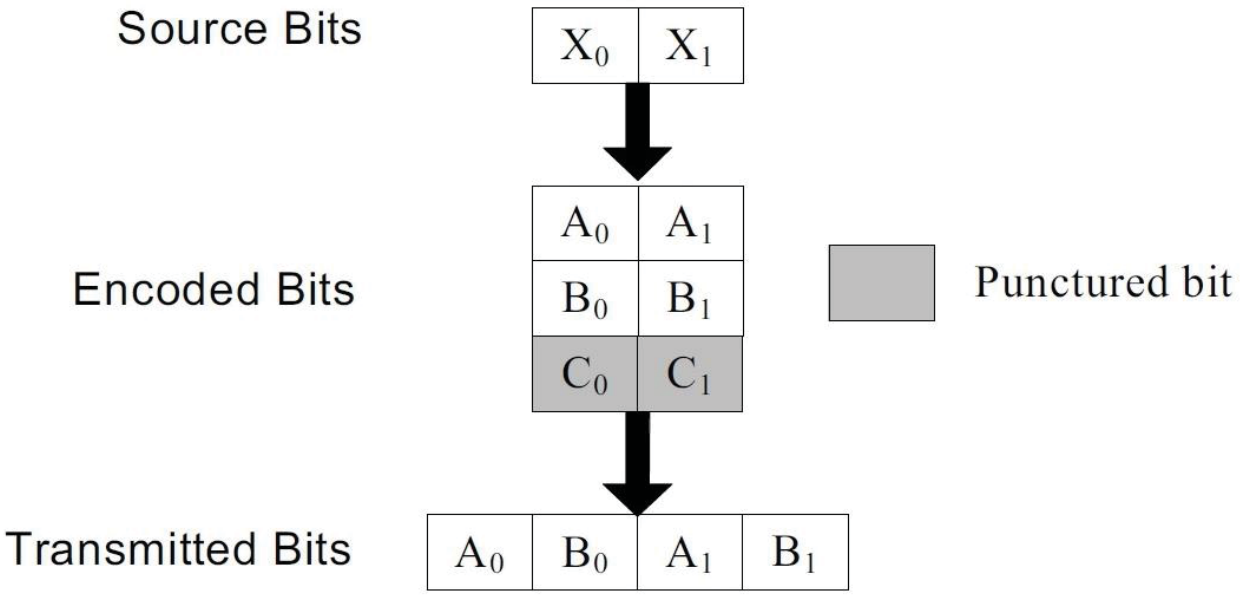

Figure 3: Puncturing pattern to obtain rate-1/2 code

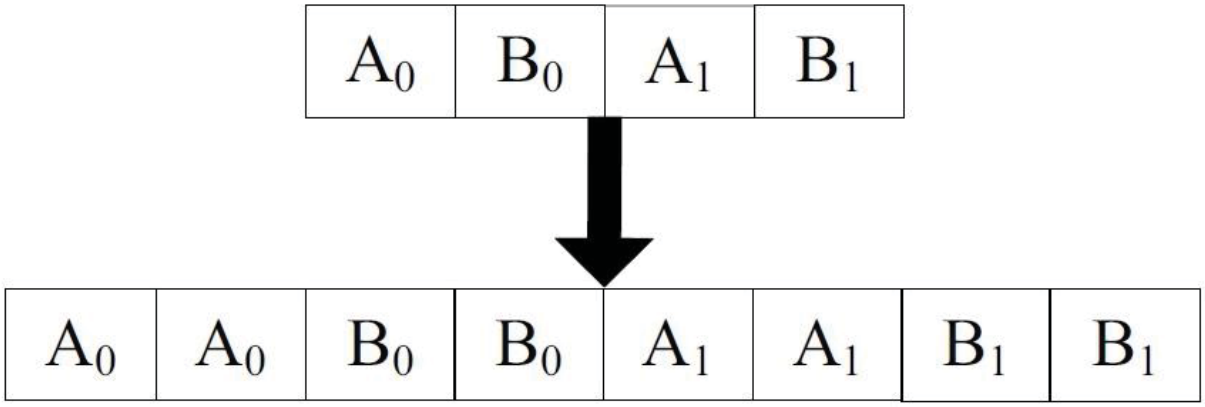

Figure 4: Repetition pattern used to obtain the effective rate-1/4 code

Rate-2/3 Code

The rate-2/3 code is obtained by puncturing the rate-1/3 mother code, as shown in Figure 5.

2.3.2 Interleaving and Puncturing

A block interleaver is used between the convolutional code and the RS code. The interleaver is of a fixed height *n* but has a flexible depth *D*, dependent on the frame size. The puncturing block is used after the interleaver in order to minimize padding overhead.

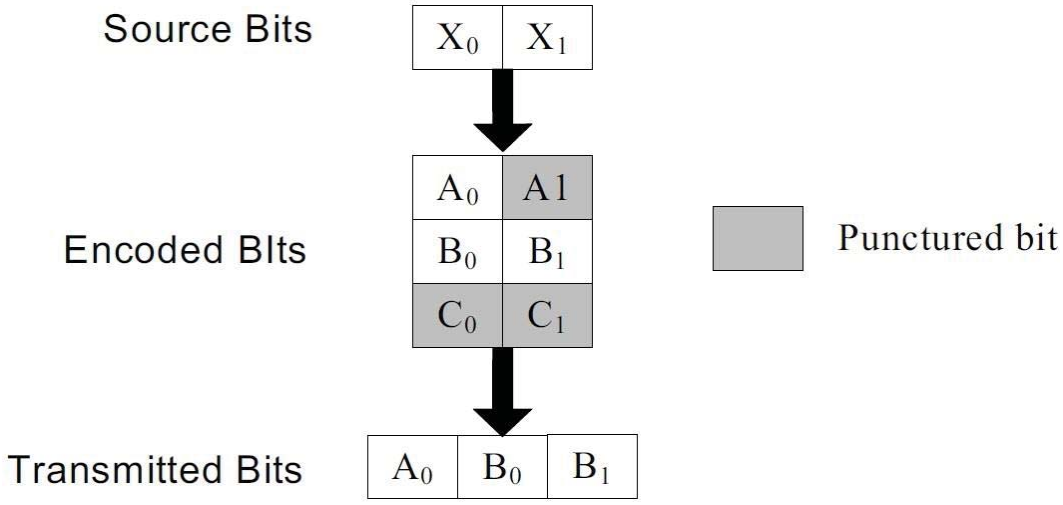

Figure 5: Puncturing pattern to obtain rate-2/3 code

2.3.3 Line Coding

Run length limited or RLL coding is a line coding technique that is used to avoid long runs of 1s and 0s that could potentially cause flicker and problems regarding recovery of the data. RLL line codes take in random data symbols at input and promise DC balance with equal 1s and 0s at the output for every symbol. In PHY I only two types of RLL coding techniques are used namely, Manchester and 4B6B, and provide tradeoffs between coding overhead and ease of implementation.

Manchester Coding

All PHY I modes, which support OOK modulation, must use Manchester coding for DC balance. The Manchester code expands each bit into an encoded 2-bit symbol as shown below.

Table 6: Manchester encoding

Bit	Manchester symbol
0	01
1	10

Table 7: Mapping 4B (input) to 6B (output)

4B (Input)	6B (Output)
0000	001110
0001	001101
0010	010011
0011	010110
0100	010101
0101	100011
0110	100110
0111	100101
1000	011001
1001	011010
1010	011100
1011	110001
1100	110010
1101	101001
1110	101010
1111	101100

4B6B Coding

All PHY I modes, which support VPPM modulation, must use 4B6B coding for DC balance. The 4B6B expands 4-bit in to 6-bit encoded symbols. The number of 1s and 0s in every VPPM encoded symbol is always equal to 3. 4B6B offers several features given below:

- In one encoded symbol duty cycle is always 50%

- DC balanced run length limiting code
- Capability of detecting errors
- Run length is limited to four

2.3.4 Modulation

On-Off Keying

On-off keying (OOK) denotes one of the simplest forms of Amplitude Shift Keying (ASK) modulation, in which bit 1 and bit 0 are represented by certain level of voltage. In OOK, ‘off’ does not certainly mean that the light is completely turned off but rather it means that the intensity of light may simply be reduced as long as one can distinguish clearly between ‘on’ and ‘off’ voltage levels.

Variable Pulse Position Modulation

The standard compliant VLC system must be able to support non-flickering, full brightness control and dimming.

As mentioned earlier, LED flickering due to VLC modulation is not suitable for eye safety. It may cause certain negative effects on humans, particularly psychological ones. In order to overcome this problem, a modulation technique is required, which supports non-flickering, since nobody wants to use a VLC system in which LED is flickering.

Another important factor is dimming. The dimming control function is a necessary requirement for LED illumination. Due to this reason a modulation technique is required, which supports dimming control function of LED light for VLC.

Another primary feature of LED illumination is providing full brightness whenever necessary or required. Hence, in order to fulfill this requirement, a modulation technique is required, which provides full brightness in terms of illumination. It is needed that VLC system must be able to support full brightness as much as LED light provides for illumination only.

VPPM provides all of these features, which makes it more reliable and feasible technique for aforementioned standard complaint VLC system. These features are non-flickering, dimming control, and full brightness. VPPM is a combination of Pulse Width Modulation (PWM) and 2-Pulse Position Modulation (2-PPM). 2-PPM provides illumination without flickering. PWM provides a control over brightness using duty cycle. VPPM equals to 2-PPM when the duty cycle of VPPM is 50%.

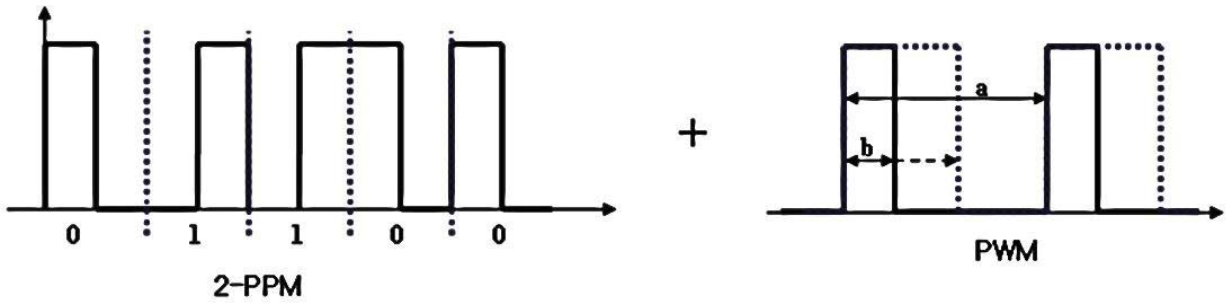

Figure 6: Basic concept of VPPM

The data mapping for VPPM is defined below. The physical value mapped from the logical data '0' has a transition from 'high' to 'low', and the physical value mapped from the logical data '1' has a transition from 'low' to 'high', as shown in Table 8. The variable *d* in Table 8 is the duty cycle of VPPM.

Table 8: Definition of data mapping for VPPM mode

Logical value	**Physical value** ***d* is the VPPM duty cycle ($0.1 \leq d \leq 0.9$)**	
0	High	$0 \leq t < dT$
	Low	$dt \leq t < T$
1	Low	$0 \leq t < (1-d)T$
	High	$(1-d)T \leq t < T$

CHAPTER

III. DESCRIPTION OF THE PROPOSED SYSTEM IMPLEMENTATION

In this chapter, we provide complete description of the proposed system implementation based on IEEE 802.15.7 standard.

3.1 System Models

IEEE 802.15.7 standard supports three system models:

- System model for PHY I
- System Model for PHY II
- System Model for PHY III

As mentioned earlier, in PHY I concatenated coding with Reed-Solomon (RS) and Convolutional Coding (CC) are used. It supports low data rates between 11.7 kbps to 266.6 kbps and is intended for outdoor usage. In PHY II only RS coding is used. It supports moderately high data rates between 1.25 Mbps and 96 Mbps and is intended for indoor usage. Both PHY I and PHY II use on-off keying (OOK) and variable pulse position modulation (VPPM) but PHY II use higher clock rates. PHY I and PHY II also support a Run Length Limited (RLL) code to provide DC balance, clock recovery, and flicker mitigation. PHY III is intended for applications with multiple light sources and detectors. It uses color shift keying (CSK) and RS coding. This type targets to achieve data rates of 12 to 96 Mbps. In this report, we are focusing on the implementation of System model for PHY I.

System Model for PHY I

System model for PHY I is divided in to two sections, which are transmitter and receiver.

The schematic diagram of the transmitter blocks (which is implemented in software) is shown in Figure 7(a). The input bits are first applied to RS encoder. In PHY I, four types of RS codes are used.

These are RS (15,11), RS (15,7), RS (15,4), and RS (15,2) with Galois field (2^4) [42]. The interleaver block between the RS code and convolutional code provides improvement in the performance. The interleaver block has fixed height *n* but has flexible depth *D*, which depends upon frame size of the data. Furthermore, in order to alleviate the burst error effect, it shuffles the data sequence. Padding overhead can be reduced by using puncturing block after interleaver [13]. The employed CC has a rate of 1/3 with constraint length K = 7. Additionally, by puncturing certain bits of the mother convolutional code with the rate of 1/3, rate-1/4 and 2/3 can be achieved. In PHY I, either Manchester encoding or 4B6B encoding is used. All OOK PHY I modes use Manchester encoding, and all other remaining VPPM PHY I modes use 4B6B encoding. Manchester code expands each bit into an encoded 2-bit symbol, while 4B6B code expands 4-bit into 6-bit encoded symbols [13].

Finally, the encoded bits are applied to the modulator. Both OOK and VPPM are supported in PHY I. In VPPM modulation, the logical data '0' has a transition from 'high' to 'low', and the logical data '1' has a transition from 'low' to 'high'. OOK represents data as either 'ON' or 'OFF'. 'ON' represents '1' and 'OFF' represents '0'.

(a)

(b)

Figure 7: Block diagram of PHY I software subsystems: (a) Transmitter (b) Receiver [43]

The block diagram of the receiver is shown in Figure 7(b). The OOK and VPPM demodulator recover and demodulate the transmitted signal. Manchester decoder is implemented by just looking at two bits at a time and marking a 'low' to 'high' transition as '0' and 'high' to 'low' transition as '1', while the

4B6B decoder is implemented using a look-up table. Sixteen 6-bit words are mapped to the corresponding 4-bit symbols. The convolutional codes are decoded using Viterbi decoder. Additionally, in order to increase the error correction capability of the Viterbi decoder, soft decision method is used. Similarly, as explained above in transmitter, deinterleaver is used to improve the performance of the design. The height *n* of the deinterleaver block is fixed but depth *D* is flexible, which is determined by the data frame size. After depuncturing, deinterleaving and zero removal steps, the RS decoder yields the recovered message bits.

3.2 Experimental Setup

The overall view of our software defined VLC experimental system is provided in Figure 8.

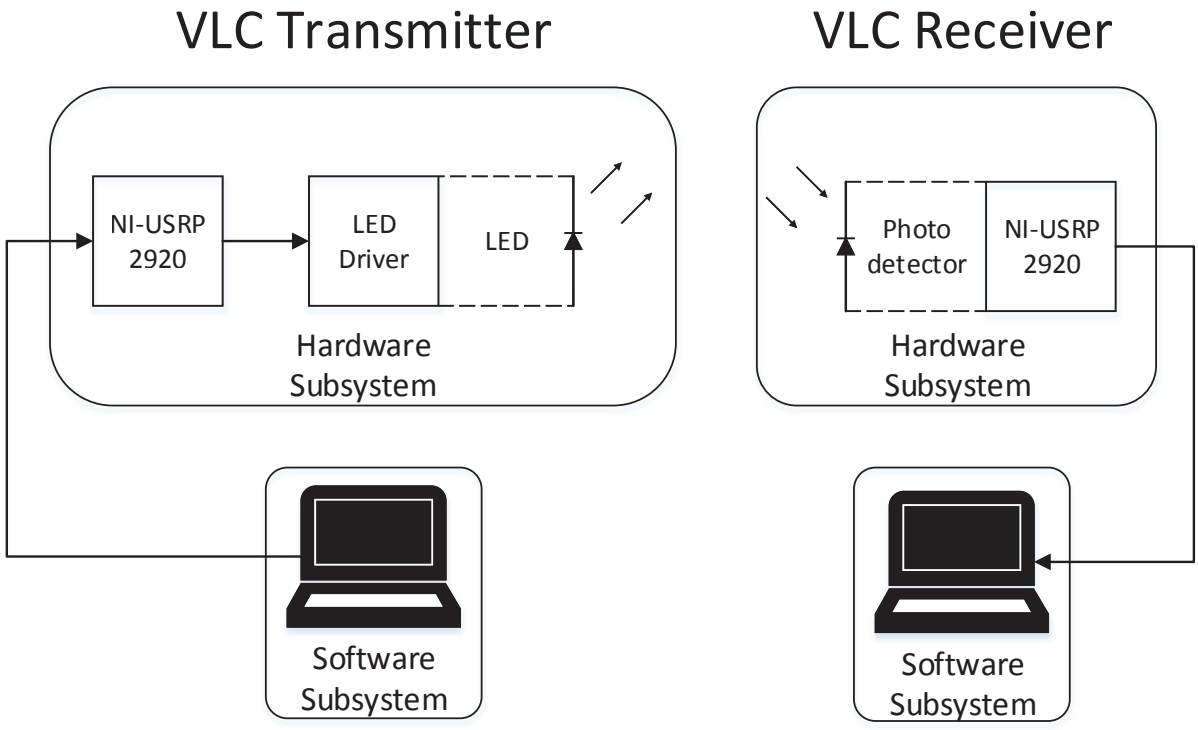

Figure 8: VLC experimental architecture [44]

3.2.1 Transmitter

On the transmitter side, a PC running LabVIEW is connected through an Ethernet port to a modified USRP 2920. In this modified USRP, we replaced the RF card with a low frequency daughter board

LFTX, which is able to produce baseband signals within the range of 0-30 MHz. In our setup, we fully implemented the transmitter blocks shown in Figure 7(a) in LabVIEW. The resulting signals are fed from the PC to the USRP. The user interface is shown in Figure 9 [44].

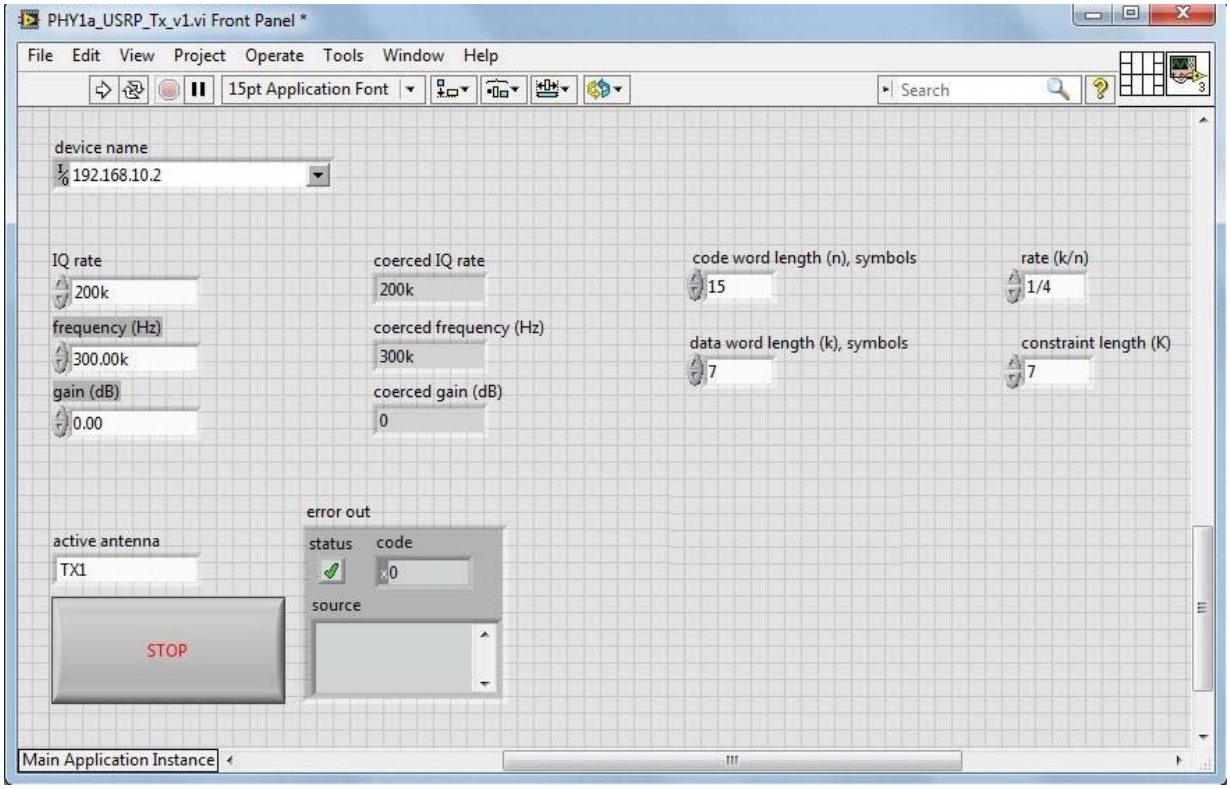

Figure 9: The LabVIEW VI for the user interface our PHY I design [44]

The digital to analog conversion of the data is implemented inside the USRP. The critical part is the optical front-end, which follows the USRP. Since the output voltage of the USRP is limited, an off-the shelf LED driver is used for biasing in order to operate within the linear range of LED (See Appendix).

We use the white LED SST-50 from Luminous. It supports a maximum power of up to 20 W and provides an extremely high output of 1150 lumens from a single chip (see Appendix).

Optical front-end configurations

There are two possible configurations of the optical front-end. One is having bias-tee and another one is without bias-tee. The implementation which is presented here in this report is without bias-tee.

Subsequently the LED driver, which is used in the implementation does not only give DC current but also capable of giving baseband modulated signal, which is fed in to LED driver, coming from USRP. Furthermore, there is no need to use a bias-tee separately, as the performance of the LED driver with a built-in bias-tee feature is much better than using bias-tee separately.

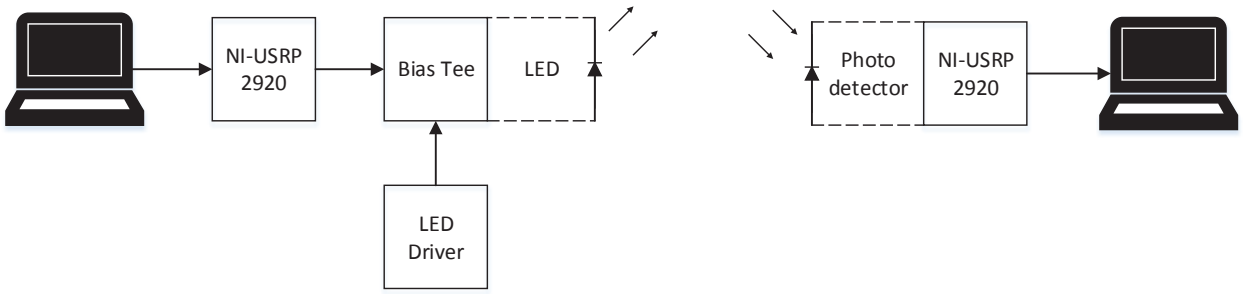

(a)

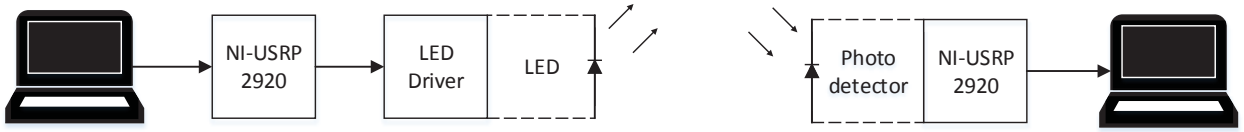

(b)

Figure 10: VLC configurations (a) with bias-tee (b) without bias-tee

3.2.2 Receiver

On the receiver side the transmitted signal is received by photodetector. The photodetector which is used in this implementation is 'PDA36A-EC' from THORLABS. The 'PDA36A-EC' has reverse-biased Positive Intrinsic Negative (PIN) diode coupled with manual switchable transimpedance amplifier (TIA) gain circuit, ranging from 0 dB to 70 dB. The photodetector has an active area of 3.6 mm x 3.6 mm (13 mm^2) and having a responsivity of 0.1A/W to 0.5A/W within visible light range (380 nm to 780 nm).

The photodetector is connected to another modified USRP with an LFRX daughter board. The analog to digital conversion takes place inside USRP. Finally, the USRP gives the data to the PC with LabVIEW where the receiver blocks shown in Figure 7(b) are fully implemented [44] (see Appendix).

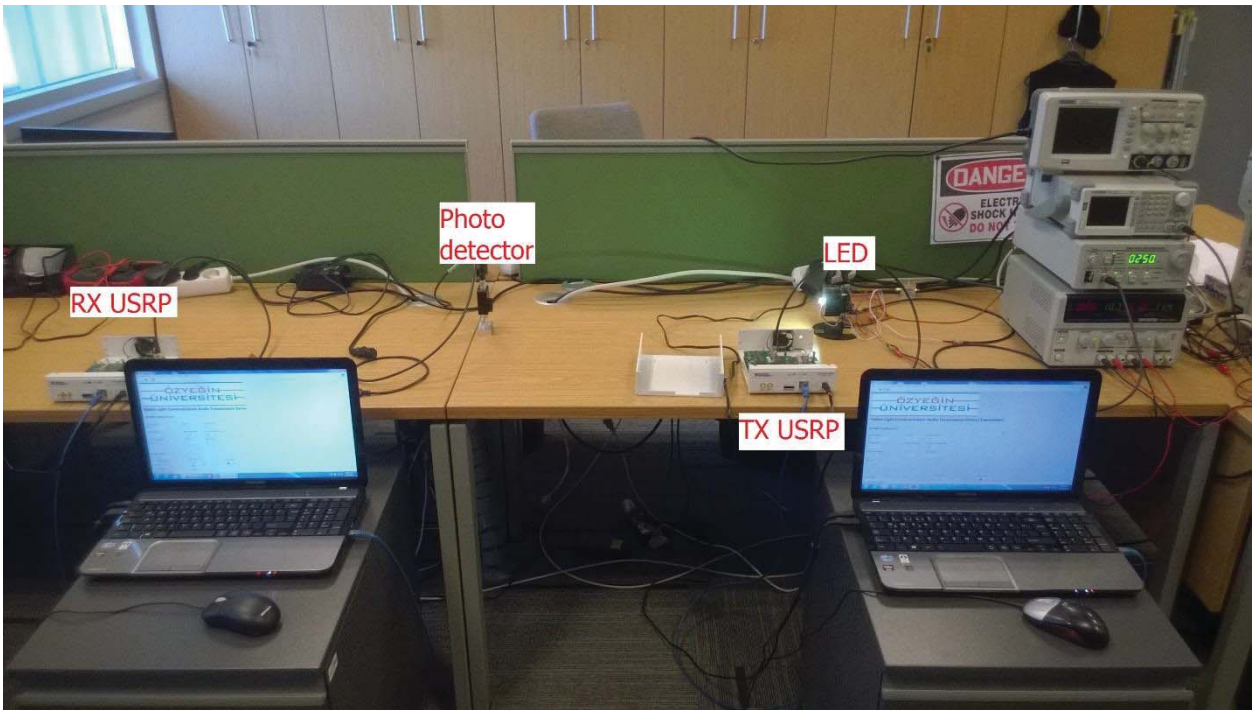

Figure 11: VLC Experimental Setup

CHAPTER

IV. EXPERIMENTAL RESULTS

In this chapter, a unique set of experimental results of the implemented physical VLC system are presented. In experiments (Exp.) 1 through 8, behavior of LED and Photodetector is evaluated using arbitrary waveform generator (AWG) instead of the USRP in the actual system. In Exp. 9, we present Bit Error Rate (BER) of the overall system for all 9 PHY I modes of IEEE 802.15.7 running on our VLC system, which operates at a distance of 1 meter. In Exp. 10 and 11, we present details of the audio streaming experiments.

Critical calculations for Exp. 1 through 8

Data rate calculation

Data rate = Input Frequency x no. of bits

Since I am transmitting 5 bits "10010" and if I have 1kHz input frequency, data rate will become 5kbps.

DC Voltage Calculation

Output DC voltage is calculated using following formula:

Vdc = (Vmax + Vmin)/2

4.1 Exp. #1: Output Vpp and Vdc versus Current (with bias-tee)

In this experiment, we vary the current on the current source (all other parameters remain constant), and we observe the output peak-to-peak voltage (Vpp) and the output DC voltage (Vdc). Note that this experiment uses the setup with the bias-tee, shown in Figure 10(a).

Data rate = 175 kbps

Input voltage (FG) = 4 Vpp

Distance between LED and Photodiode = 20 cm

Photodiode gain = 30 dB

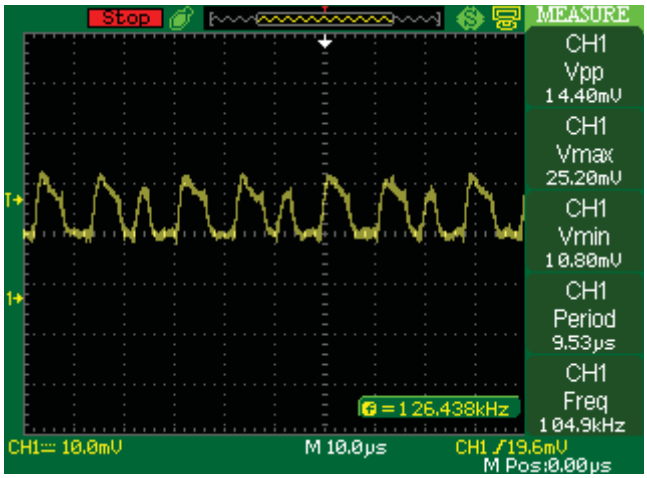

Figure 12: Input current 20 mA

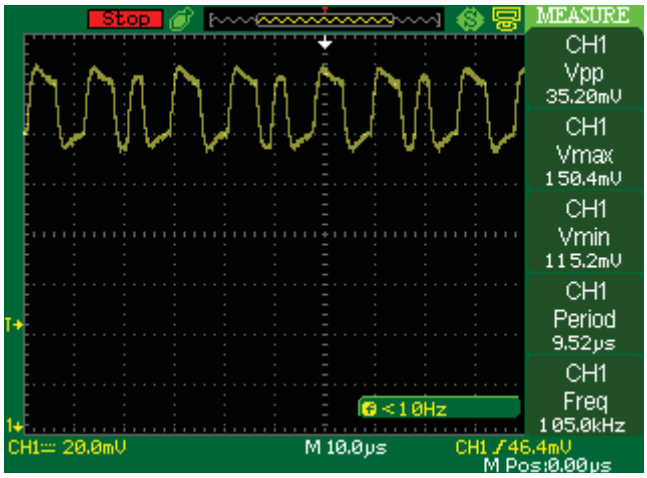

Figure 13: Input current 200 mA

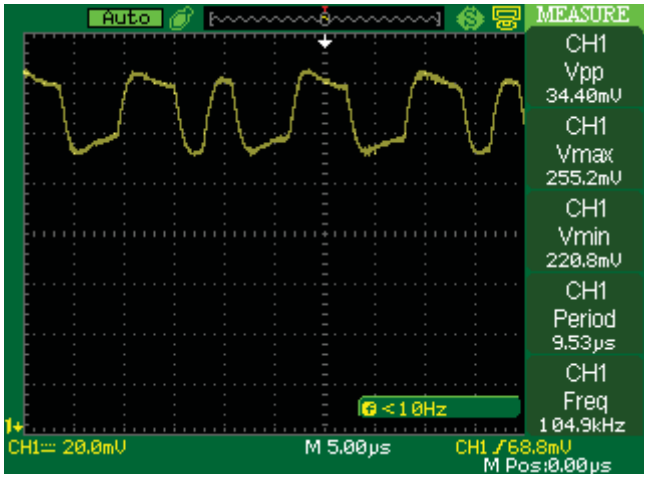

Figure 14: Input current 320 mA

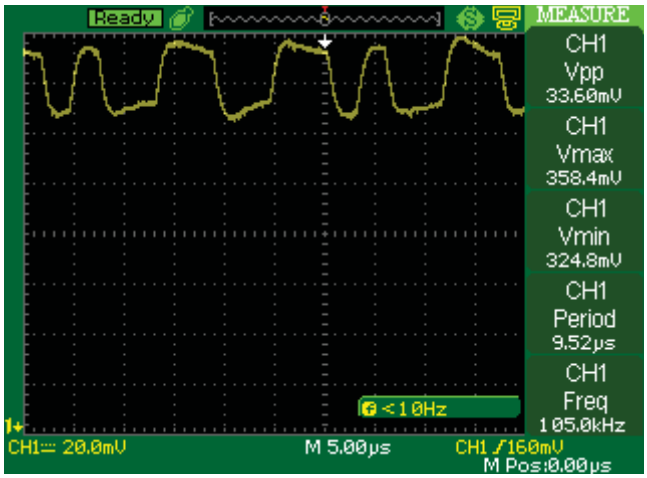

Figure 15: Input current 480 mA

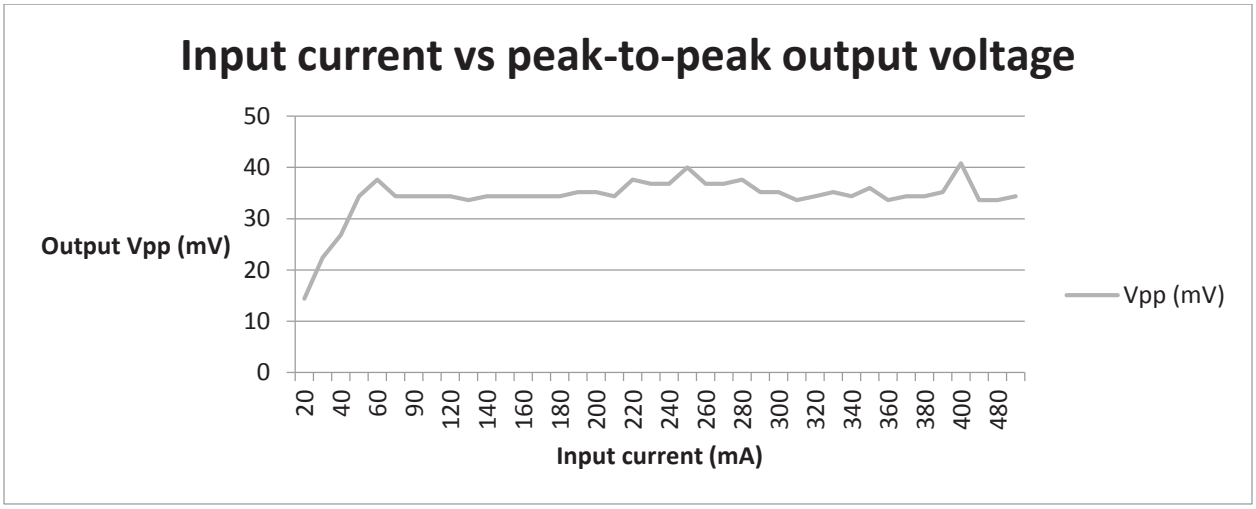

Figure 16: Graph of peak-to-peak output voltage vs input current

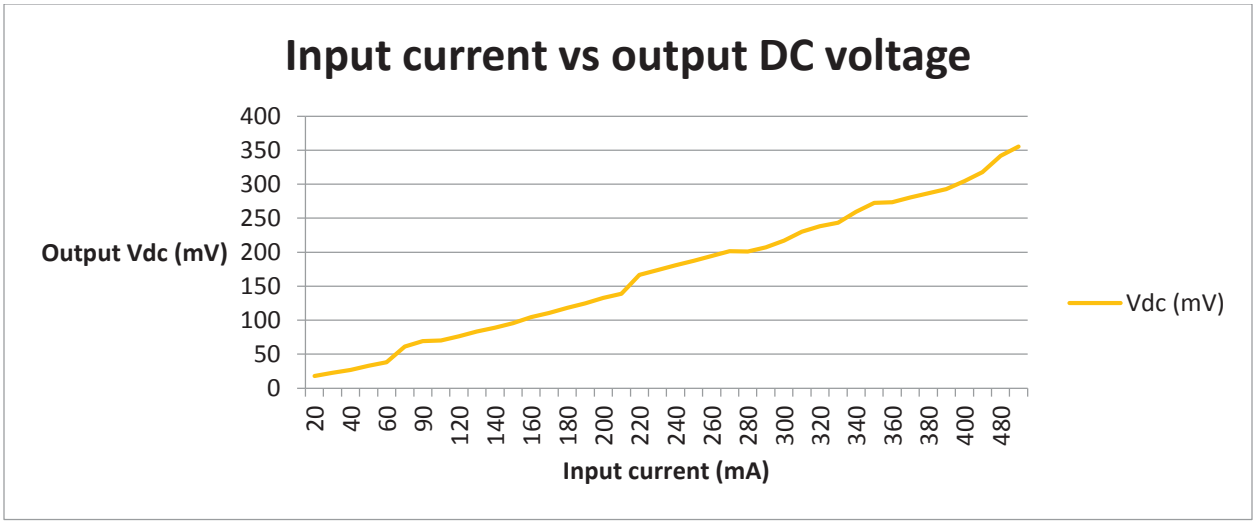

Figure 17: Graph of output DC voltage vs input current

Results:

- Peak-to-peak output voltage initially increases but after 30mV it does not change much.
- Output DC voltage increases with the increase in input current.

4.2 Exp. #2: Output Vpp and Vdc versus Frequency (with bias-tee)

In this experiment, we vary the frequency (data rate) on AWG (all other parameters remain constant), and we observe the output Vpp and the output Vdc. Note that this experiment uses the setup with the bias-tee, shown in Figure 10(a).

Input current = 250 mA

Input voltage (FG) = 4 Vpp

Distance between LED and Photodiode = 20 cm

Photodiode gain = 30 dB

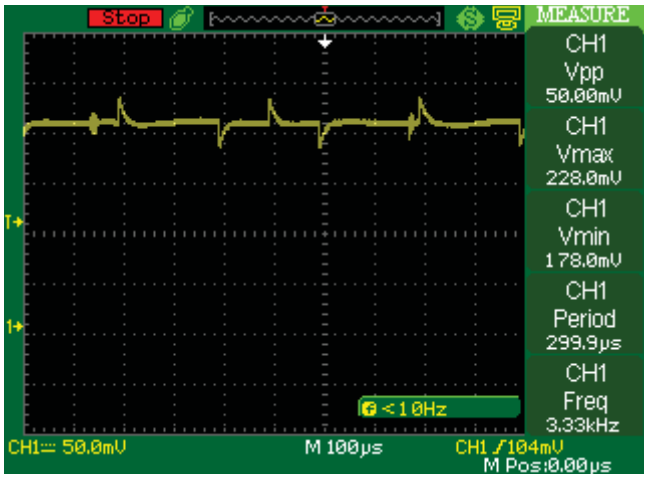

Figure 18: Input frequency 1 kHz (data rate 5 kbps)

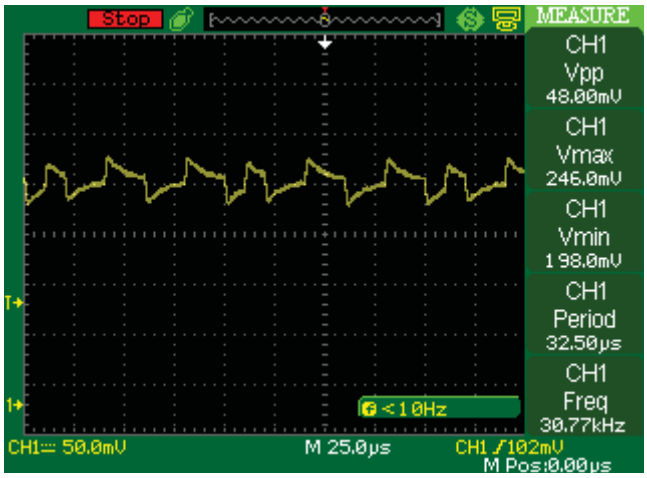

Figure 19: Input frequency 10 kHz (data rate 50 kbps)

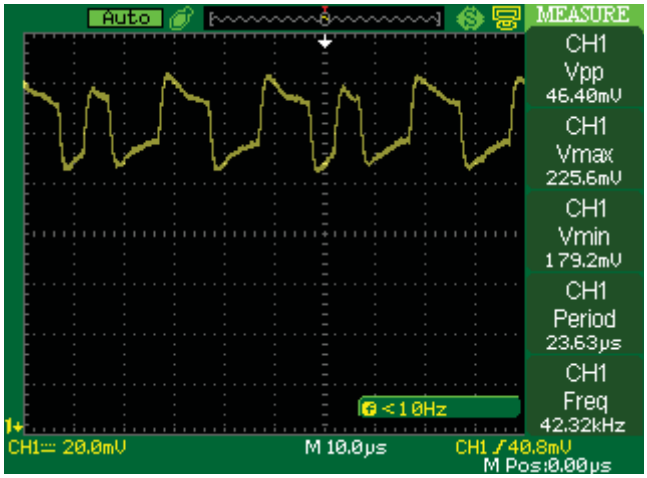

Figure 20: Input frequency 20 kHz (data rate 100 kbps)

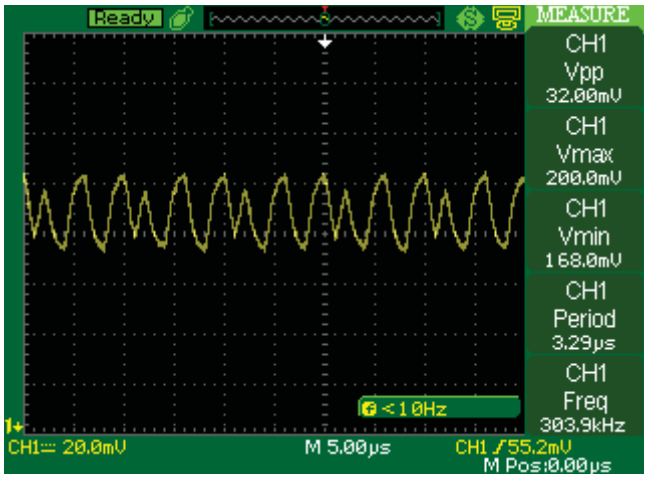

Figure 21: Input frequency 100 kHz (data rate 500 kbps)

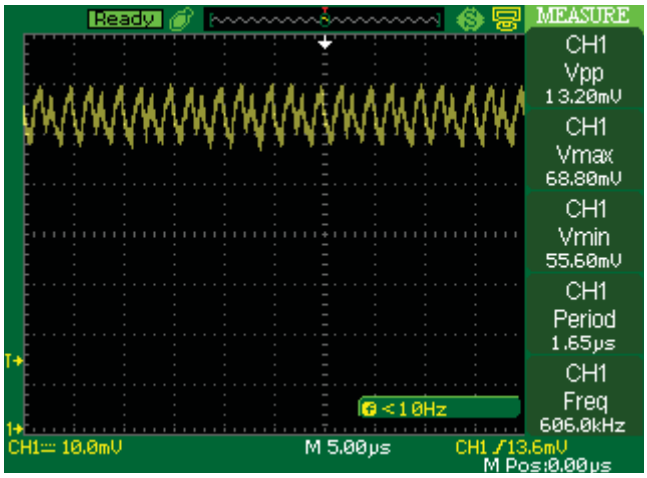

Figure 22: Input frequency 200 kHz (data rate 1000 kbps)

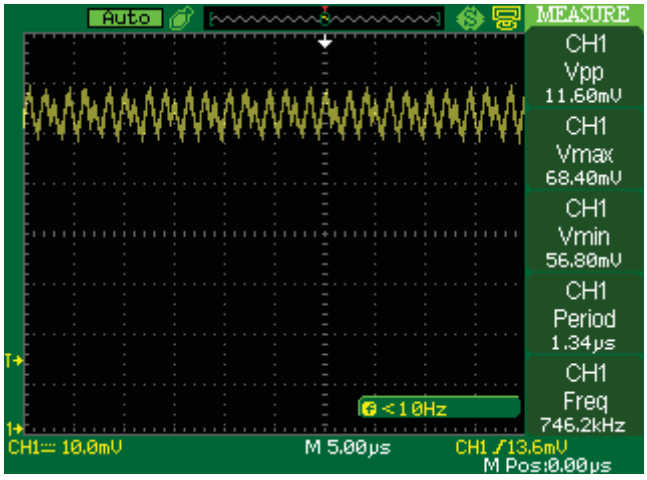

Figure 23: Input frequency 250 kHz (data rate 1250 kbps)

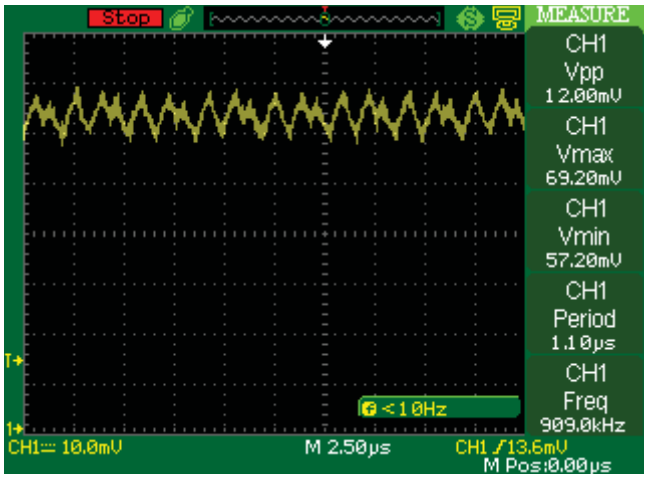

Figure 24: Input frequency 300 kHz (data rate 1500 kbps)

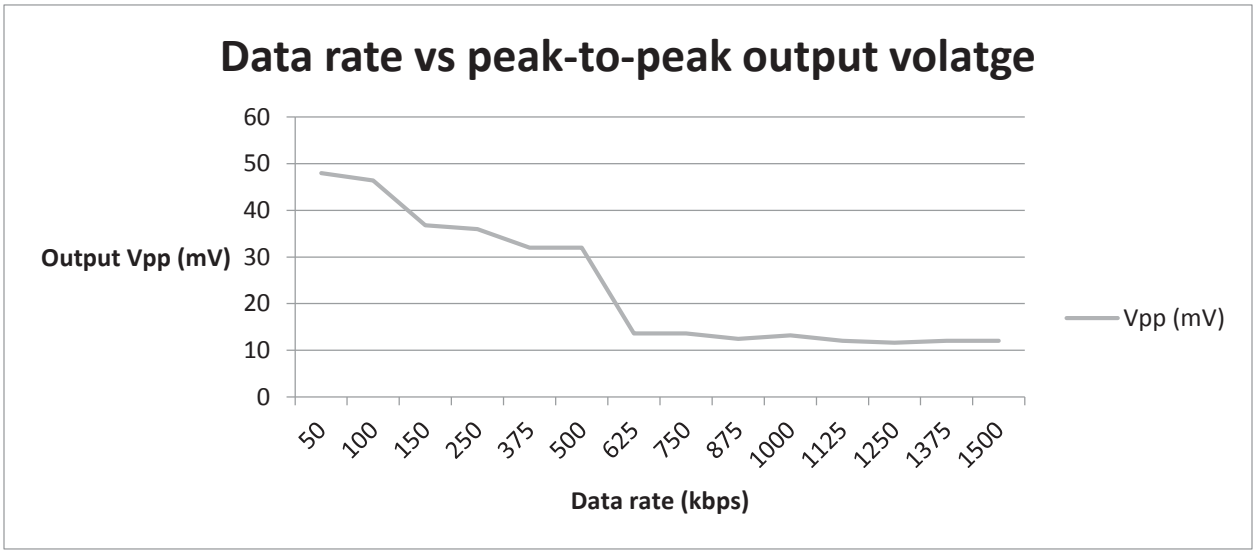

Figure 25: Graph of peak-to-peak output voltage vs input data rate (frequency)

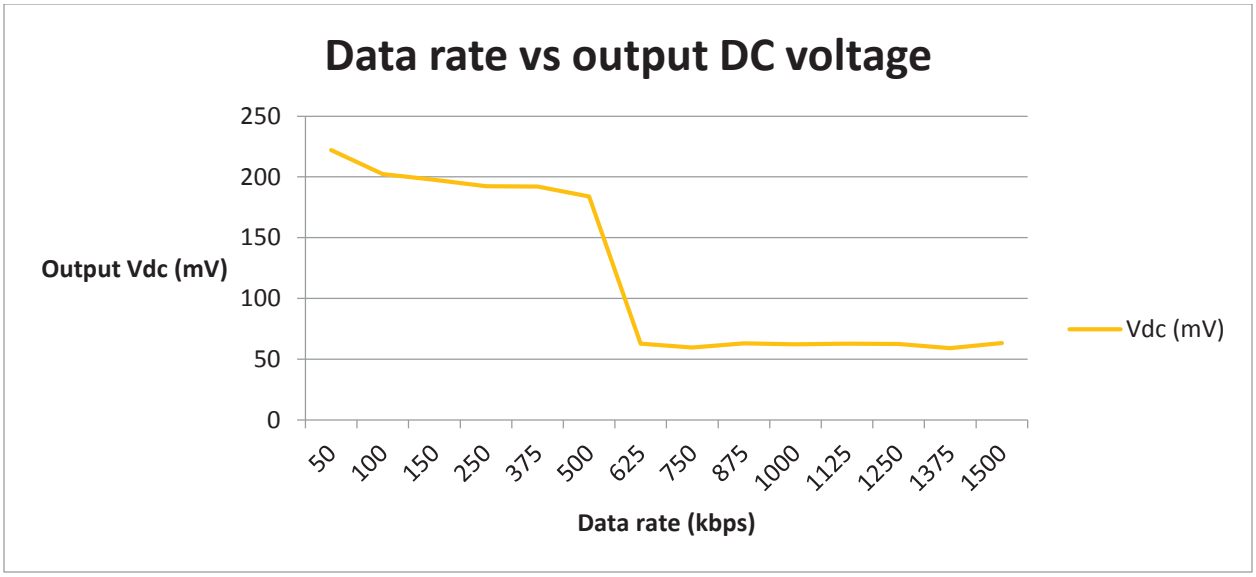

Figure 26: Graph of output DC voltage vs input data rate (frequency)

Results:

- Peak-to-peak output voltage decreases with the increase in data rate.
- Output DC voltage decreases with the increase in data rate.

4.3 Exp. #3: Output Vpp and Vdc versus Input Vpp (with bias-tee)

In this experiment, we vary the Vpp on AWG (all other parameters remain constant), and we observe the output Vpp and the output Vdc. Note that this experiment uses the setup with the bias-tee, shown in Figure 10(a).

Input current = 250 mA

Photo detector gain = 30 dB

Data rate = 250 kbps

Distance between LED and Photodiode = 20 cm

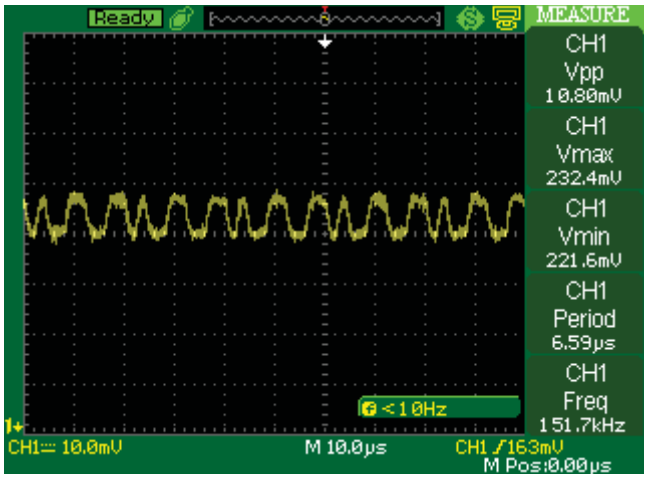

Figure 27: Input voltage of 1 Vpp

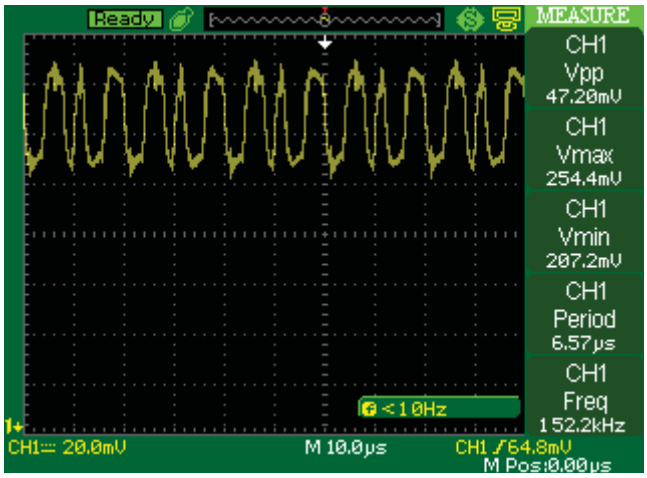

Figure 28: Input voltage of 5 Vpp

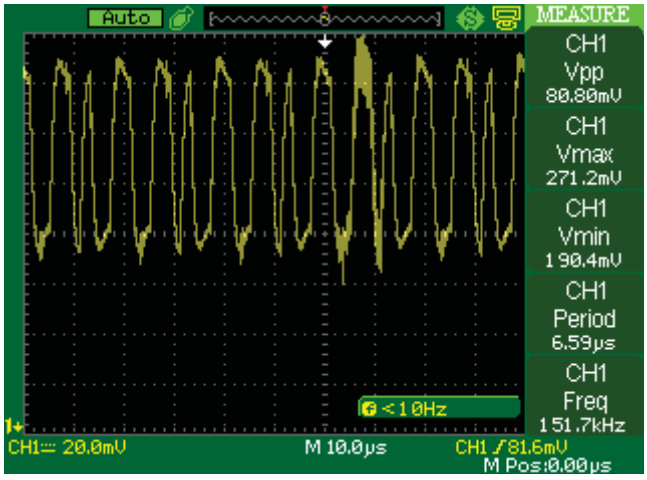

Figure 29: Input voltage of 10 Vpp

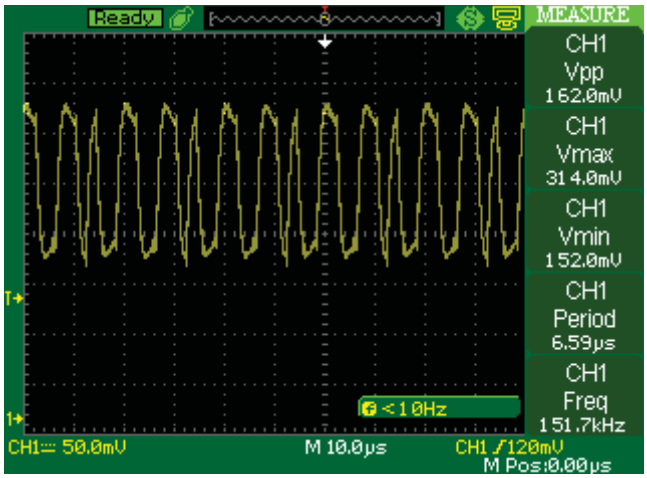

Figure 30: Input voltage of 20 Vpp

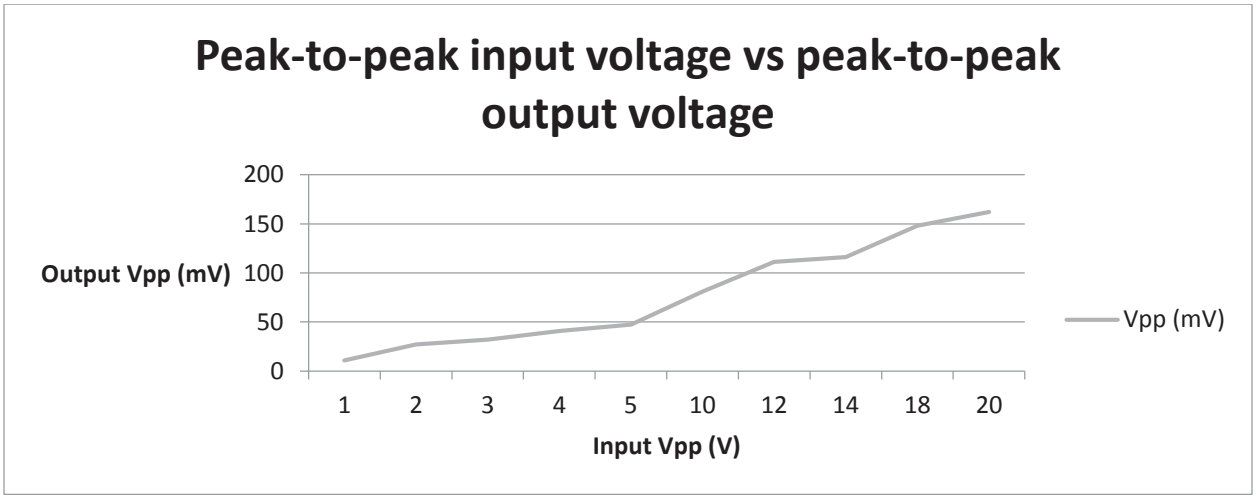

Figure 31: Peak-to-peak output voltage vs peak-to-peak input voltage

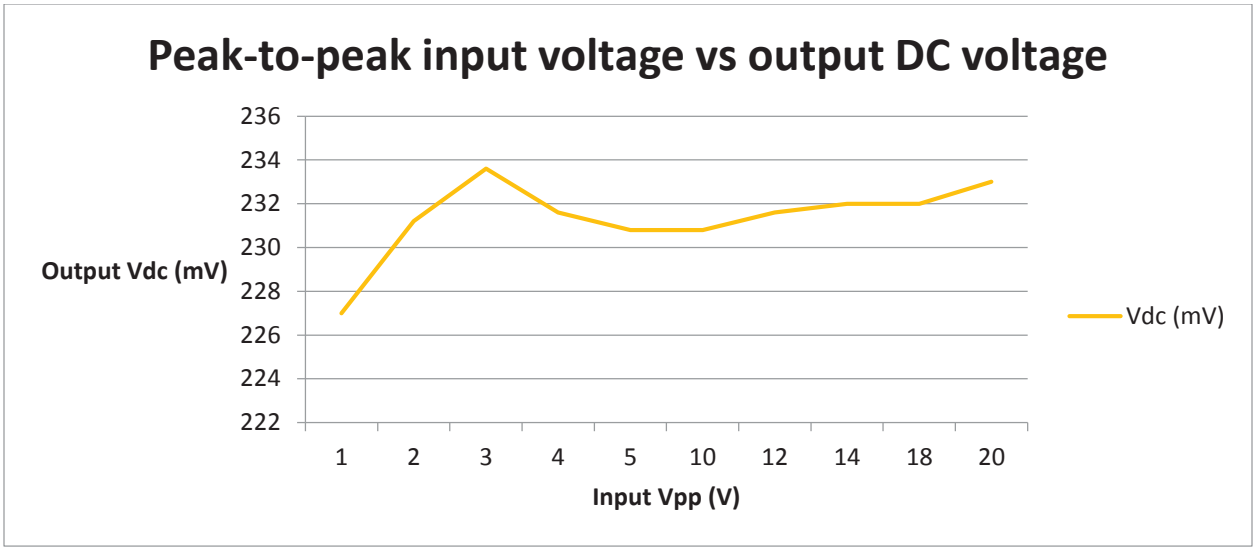

Figure 32: Output DC voltage vs peak-to-peak input voltage

Results:

- Peak-to-peak output voltage increases with the increase in peak-to-peak input voltage.
- Output DC voltage increases a little bit with the increase in peak-to-peak input voltage.

4.4 Exp. #4: Max Distance versus Input Vpp (with bias-tee)

In this experiment, we vary Vpp on AWG (all other parameters except distance remain constant), and we increase the distance between the LED and the photodetector up to a distance (which we call max distance) when the received signal is not intelligible. Note that this experiment uses the setup with the bias-tee, shown in Figure 10(a).

Input current = 500 mA

Photo detector gain = 30 dB, but at 200 kHz change it to 20 dB

Data rate = 50 kbps

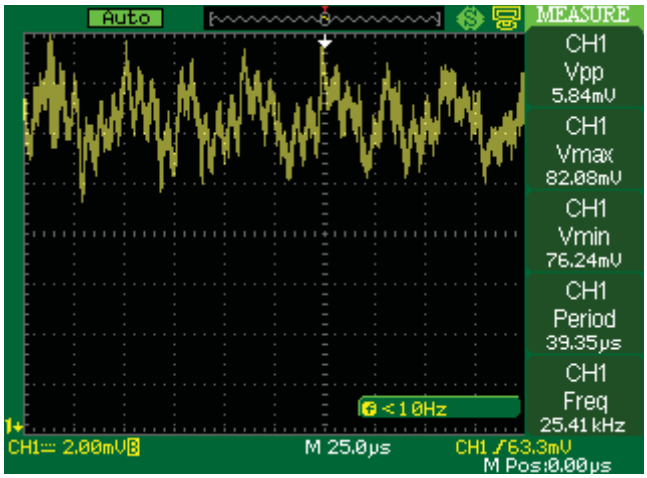

Figure 33: 2Vpp_10kHz(50kbps)_50cm

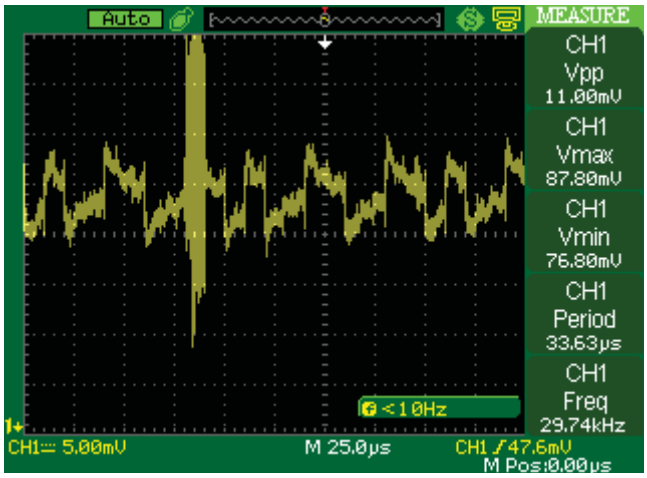

Figure 34: 5Vpp_10kHz(50kbps)_62cm

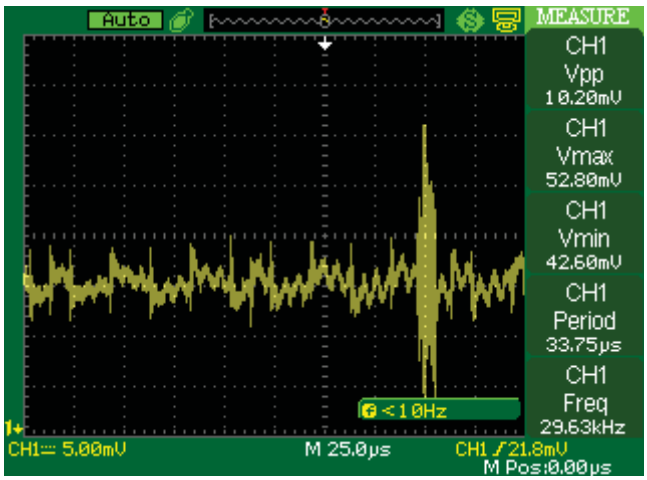

Figure 35: 10Vpp_10kHz(50kbps)_110cm

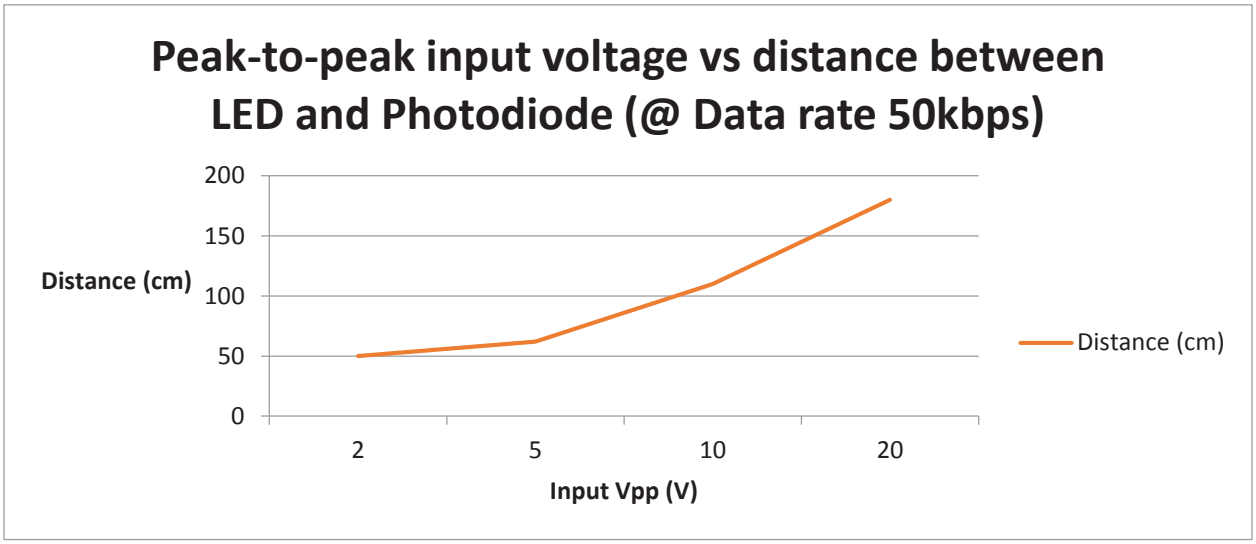

Figure 36: Distance vs peak-to-peak input voltage

Results:

- Distance increases with the increase in peak-to-peak input voltage at same data rate.

4.5 Exp. #5: Max Distance versus Frequency (with bias-tee)

In this experiment, we vary the frequency on AWG (all other parameters except distance remain constant), and we increase the distance between the LED and the photodetector up to a distance when the received signal is not intelligible. Note that this experiment uses the setup with the bias-tee, shown in Figure 10(a).

Input current = 500 mA

Photo detector gain = 30 dB, but at 200 kHz change it to 20 dB

Input voltage (FG) = 20 Vpp

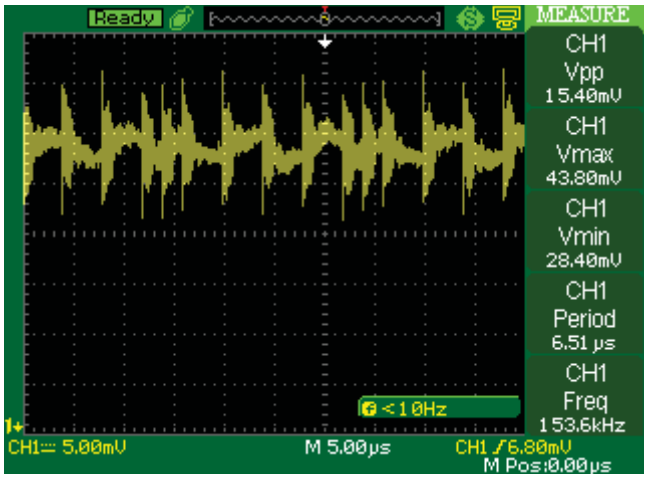

Figure 37: 20Vpp_50kHz(250kbps)_180cm

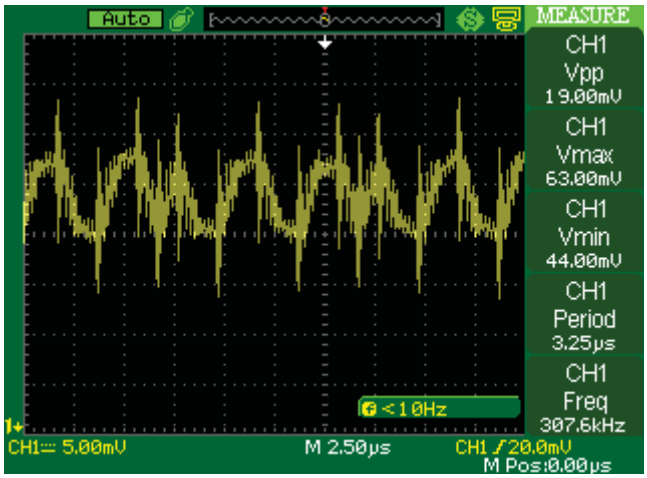

Figure 38: 20Vpp_100kHz(500kbps)_80cm

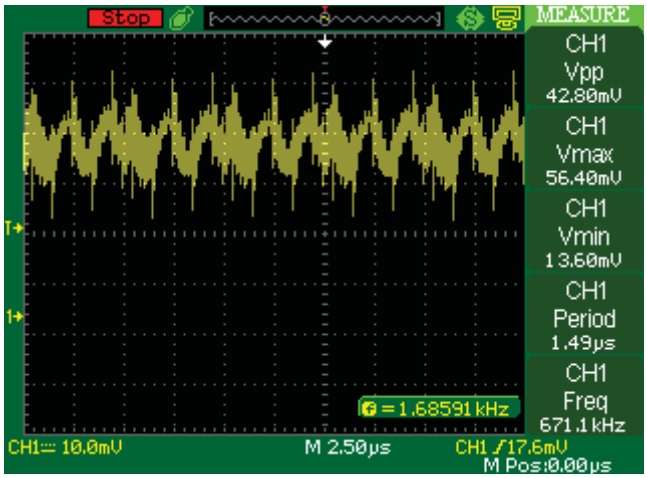

Figure 39: 20Vpp_200kHz(1000kbps)_40cm

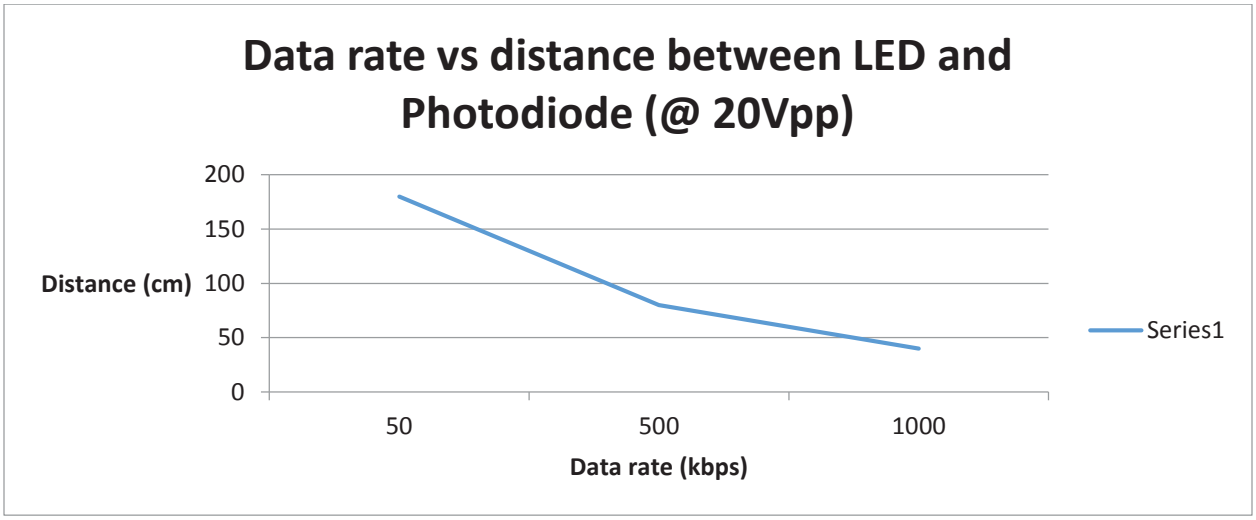

Figure 40: Distance vs data rate (frequency)

Results:

- Distance decreases with the increase in data rate at same peak-to-peak input voltage.

4.6 Exp. #6: Output Vpp and Vdc versus Current (without bias-tee)

In this experiment, we vary the current on the current source (all other parameters remain constant), and we observe the output peak-to-peak voltage (Vpp) and the output DC voltage (Vdc). Note that this experiment uses the setup without bias-tee, shown in Figure 10(b).

Data rate = 250 kbps

Input voltage (FG) = 4 Vpp

Distance between LED and Photodiode = 20 cm

Photodiode gain = 30 dB

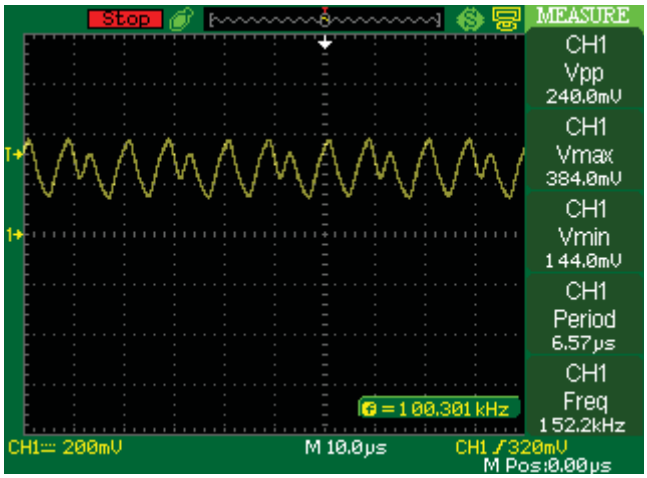

Figure 41: Input current 20 mA

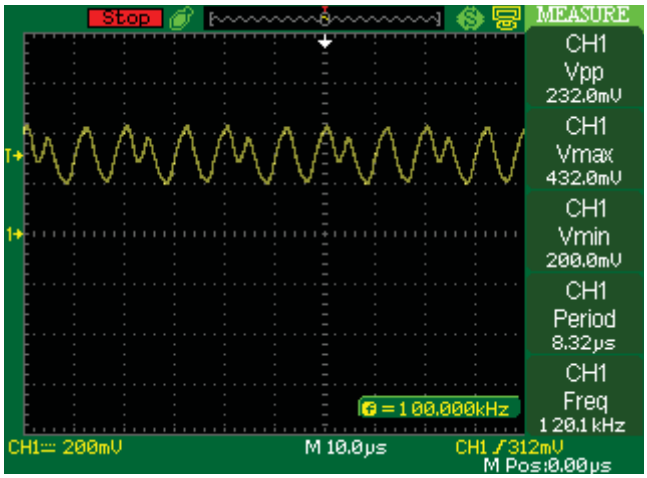

Figure 42: Input current 100 mA

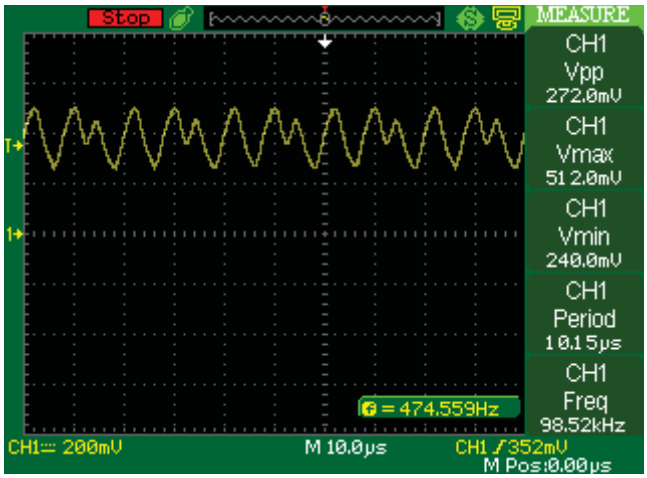

Figure 43: Input current 200 mA

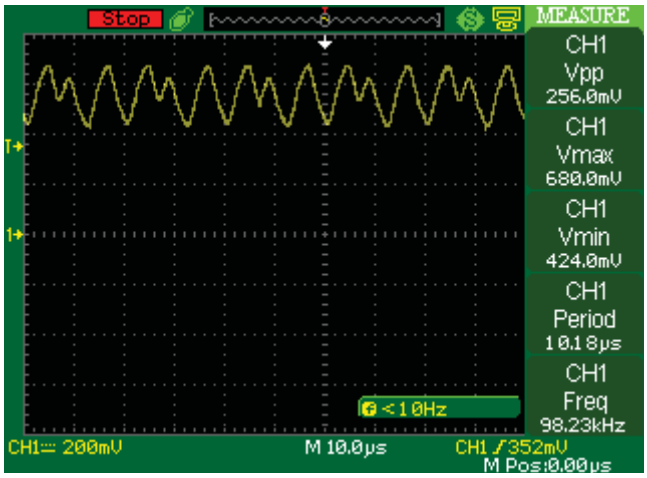

Figure 44: Input current 450 mA

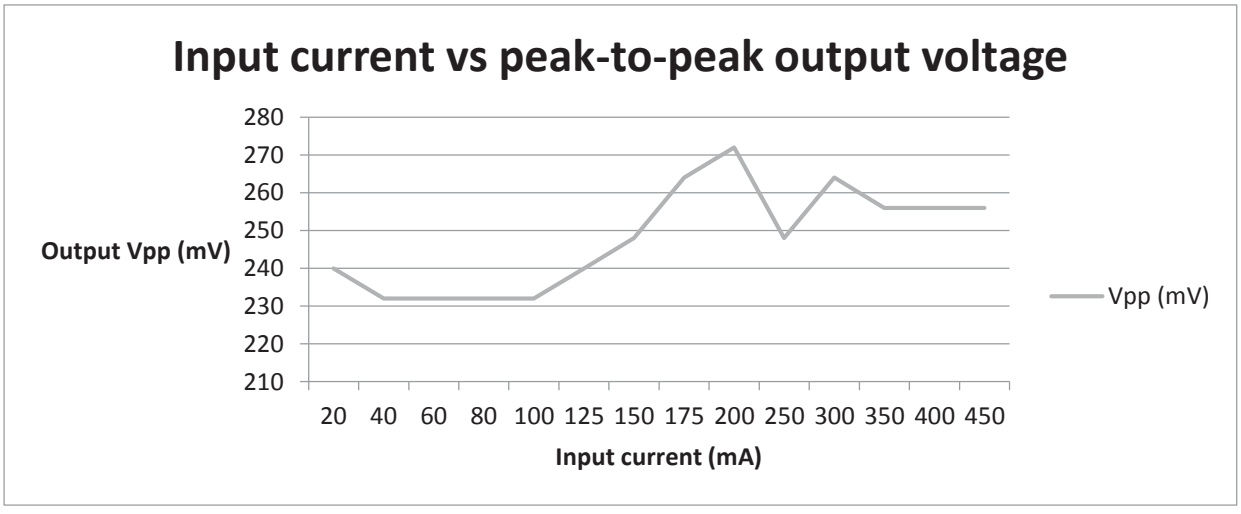

Figure 45: Peak-to-peak output voltage vs input current

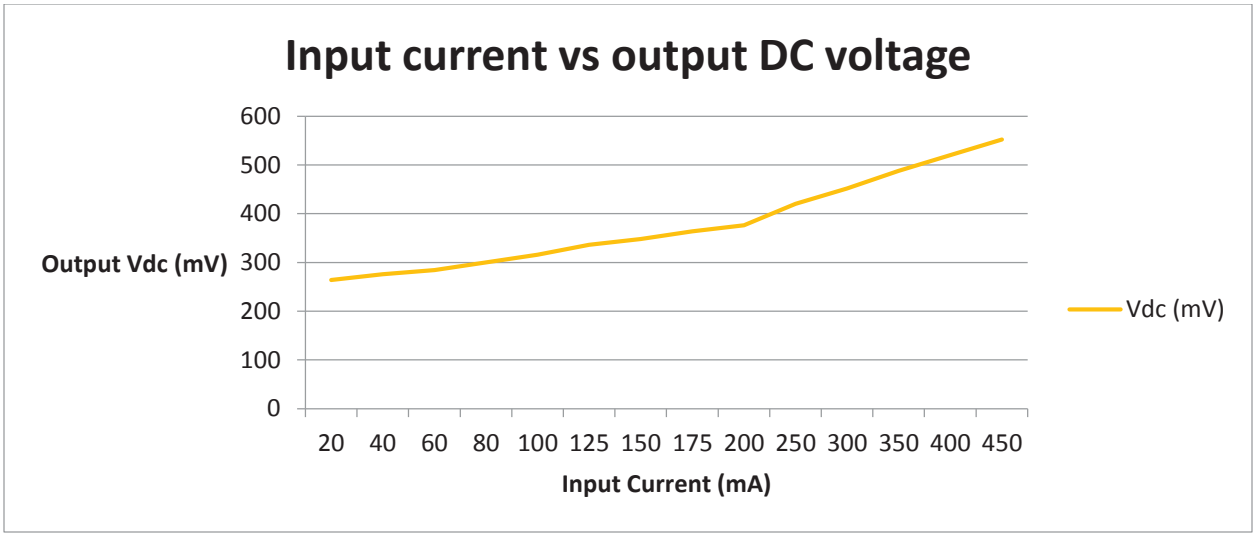

Figure 46: Output DC voltage vs input current

Results:

- Peak-to-peak voltage initially increases with the increase in current, but after 200 mA it does not increase.
- Output DC voltage increases with the increase in input current.

4.7 Exp. #7: Output Vpp and Vdc versus Frequency (without bias-tee)

In this experiment, we vary the frequency (data rate) on AWG (all other parameters remain constant), and we observe the output peak-to-peak voltage (Vpp) and the output DC voltage (Vdc). Note that this experiment uses the setup without bias-tee, shown in Figure 10(b).

Input current from current source = 250 mA

Input voltage (FG) = 4 Vpp

Distance between LED and Photodiode = 20 cm

Photodiode gain = 30 dB, but at 200 kHz change it to 20 dB

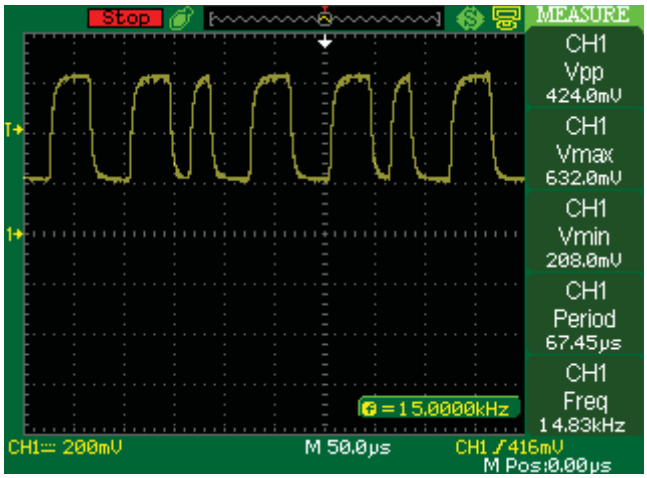

Figure 47: Input frequency 5 kHz (data rate 25 kbps)

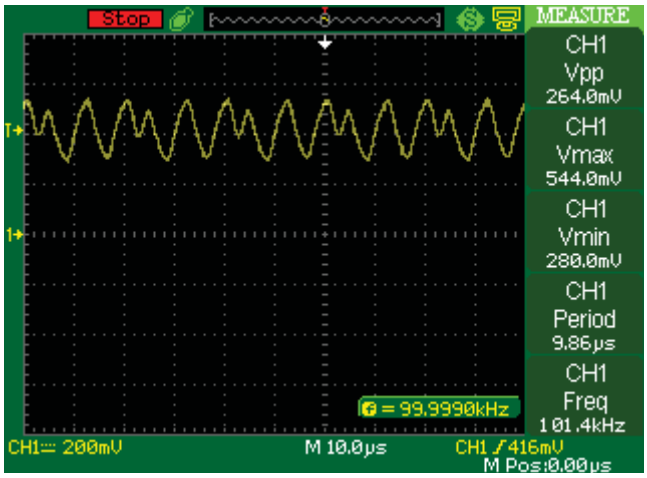

Figure 48: Input frequency 50 kHz (data rate 250 kbps)

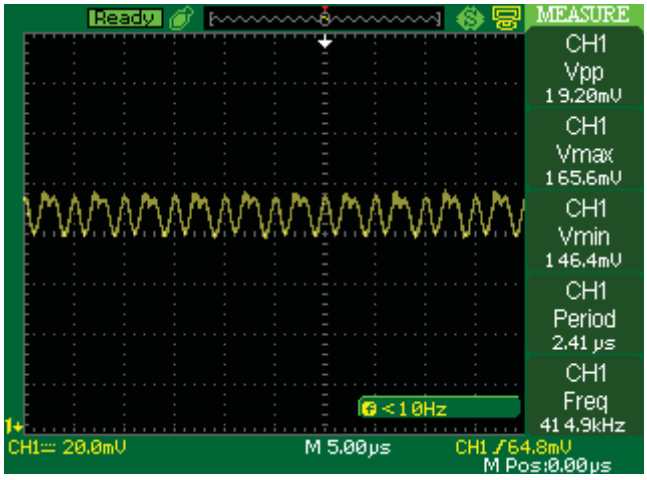

Figure 49: Input frequency 200 kHz (data rate 1000 kbps)

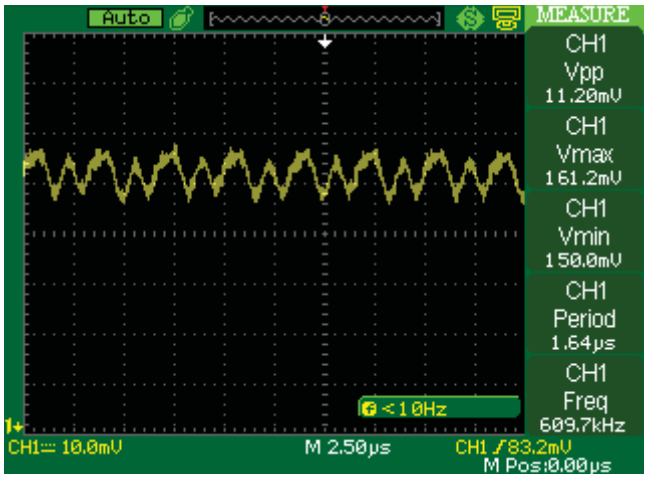

Figure 50: Input frequency 300 kHz (data rate 1500 kbps)

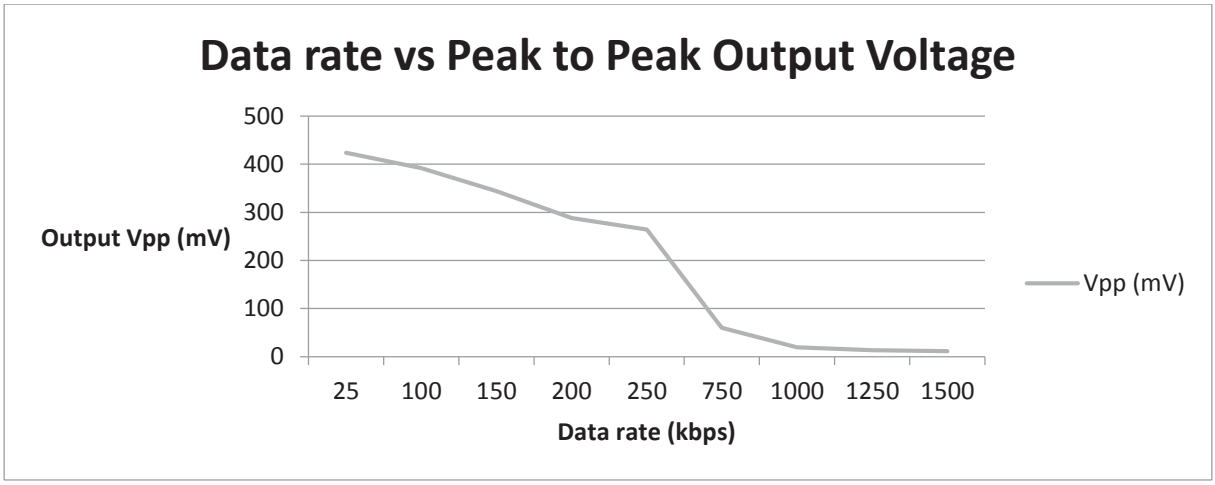

Figure 51: Peak-to-peak output voltage vs data rate (frequency)

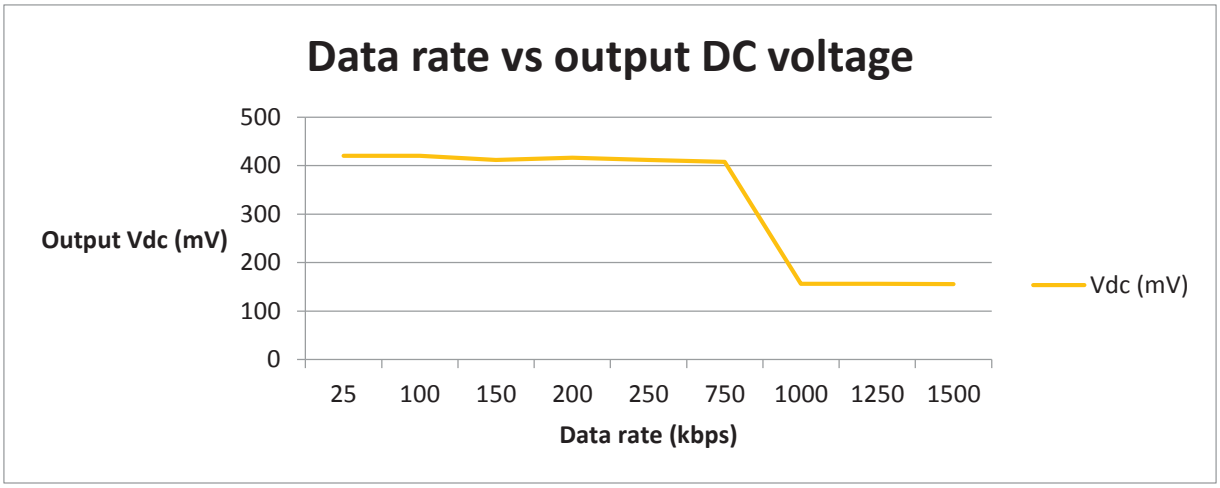

Figure 52: Output DC voltage vs data rate (frequency)

Results:

- Peak-to-peak output voltage decreases with the increase in data rate.
- Output DC voltage decreases with the increase in data rate.

4.8 Exp. #8: Output Vpp and Vdc versus Input Vpp (without bias-tee)

In this experiment, we vary the Vpp on AWG (all other parameters remain constant), and we observe the output peak-to-peak voltage (Vpp) and the output DC voltage (Vdc). Note that this experiment uses the setup without bias-tee, shown in Figure 10(b).

Input current from current source = 250 mA

Data rate = 250 kbps

Distance between LED and Photodiode = 20 cm

Photodiode gain = 30 dB

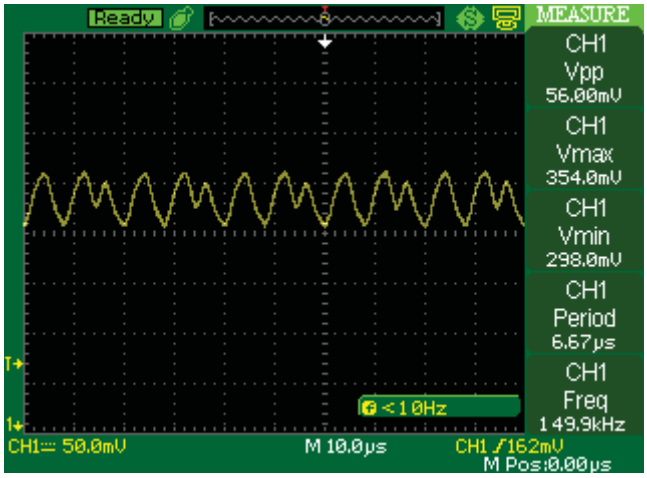

Figure 53: Input voltage of 1 Vpp

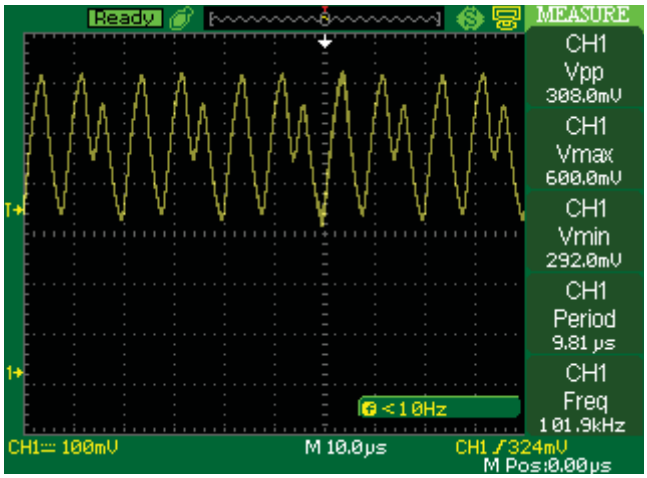

Figure 54: Input voltage of 5 Vpp

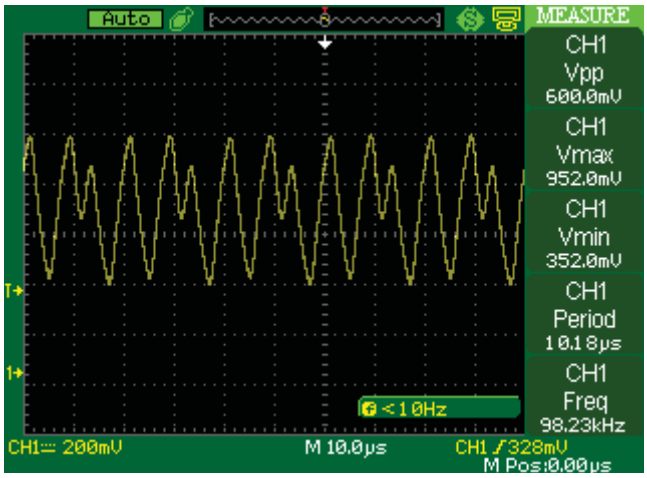

Figure 55: Input voltage of 10 Vpp

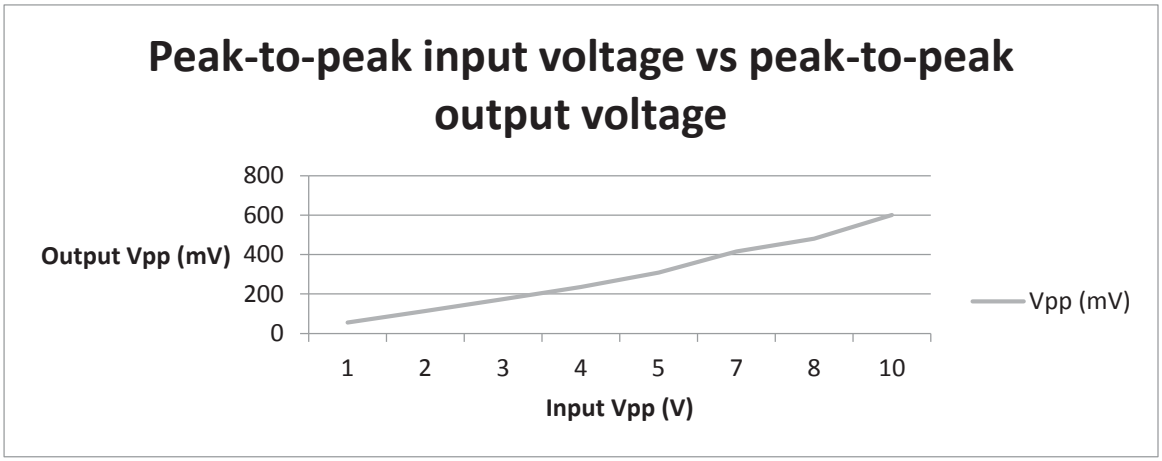

Figure 56: Graph of peak-to-peak input voltage vs peak-to-peak output voltage

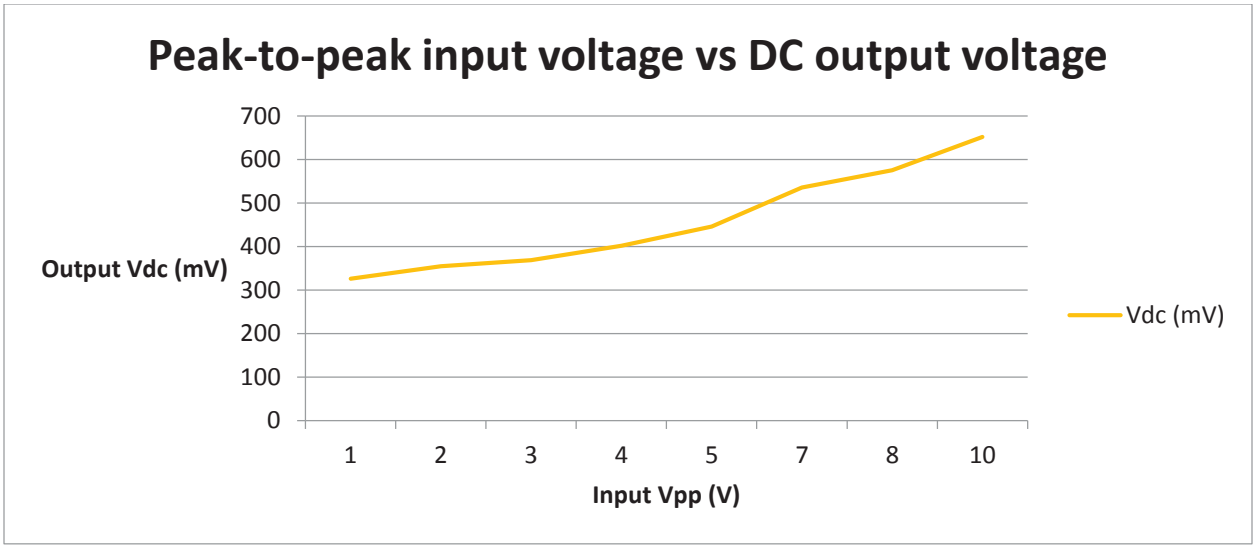

Figure 57: Peak-to-peak input voltage vs DC output voltage

Results:

- Peak-to-peak output voltage increase with the increase in peak-to-peak input voltage.
- Output DC voltage increases with the increase in peak-to-peak input voltage.

4.9 Exp. #9: BER Measurements (without bias-tee)

In this experiment, we present bit error rate (BER) results of all PHY I modes of IEEE 802.15.7 running on our VLC system, which operates at a distance of 1 meter. In BER measurements, a pseudorandom binary sequence generator is used as the source. Figure 58 provides BER results of modes PHY I.a to PHY I.e, which are based on OOK and Figure 59 provides BER results of modes PHY I. f to PHY I.g which use VPPM. The BER is plotted versus illuminance (somewhat correlates with SNR), which is adjusted through LED driver. In both Figure 59 and Figure 60, it is observed that with the increase in illuminance, BER performance first significantly improves, and then becomes saturated, i.e., becomes constant. As mentioned earlier the output of the USRP is fed in to LED driver, due to output voltage limitation of the USRP.

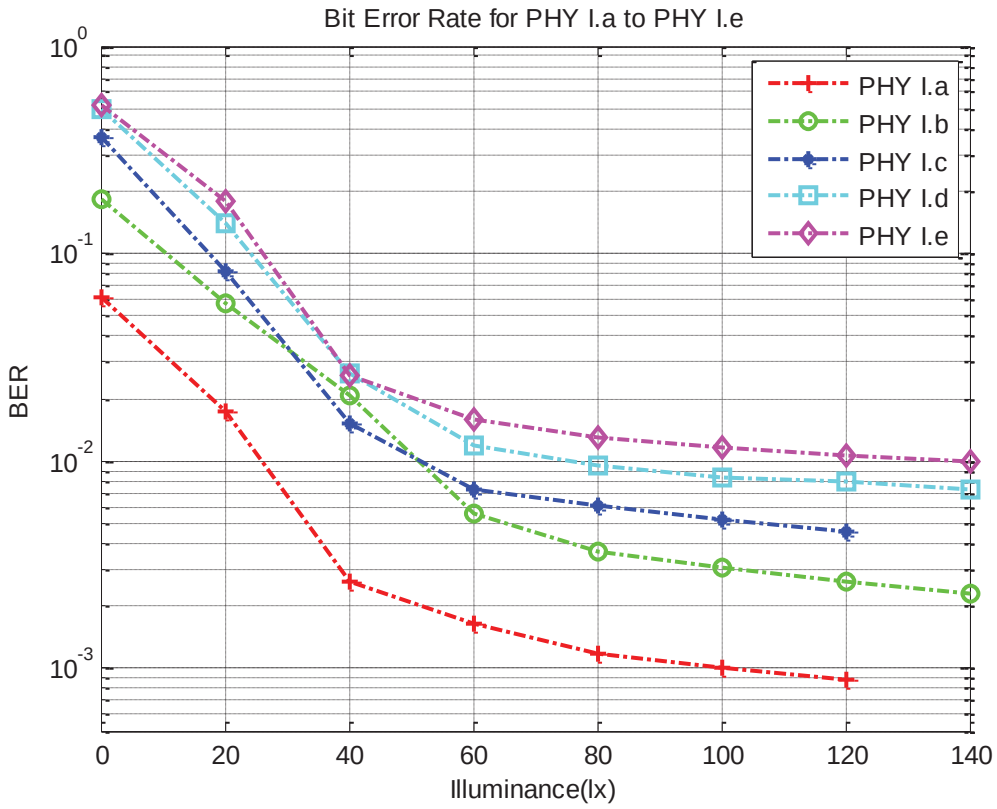

Figure 58: BER VLC HW results of PHY I.a to PHY I.e

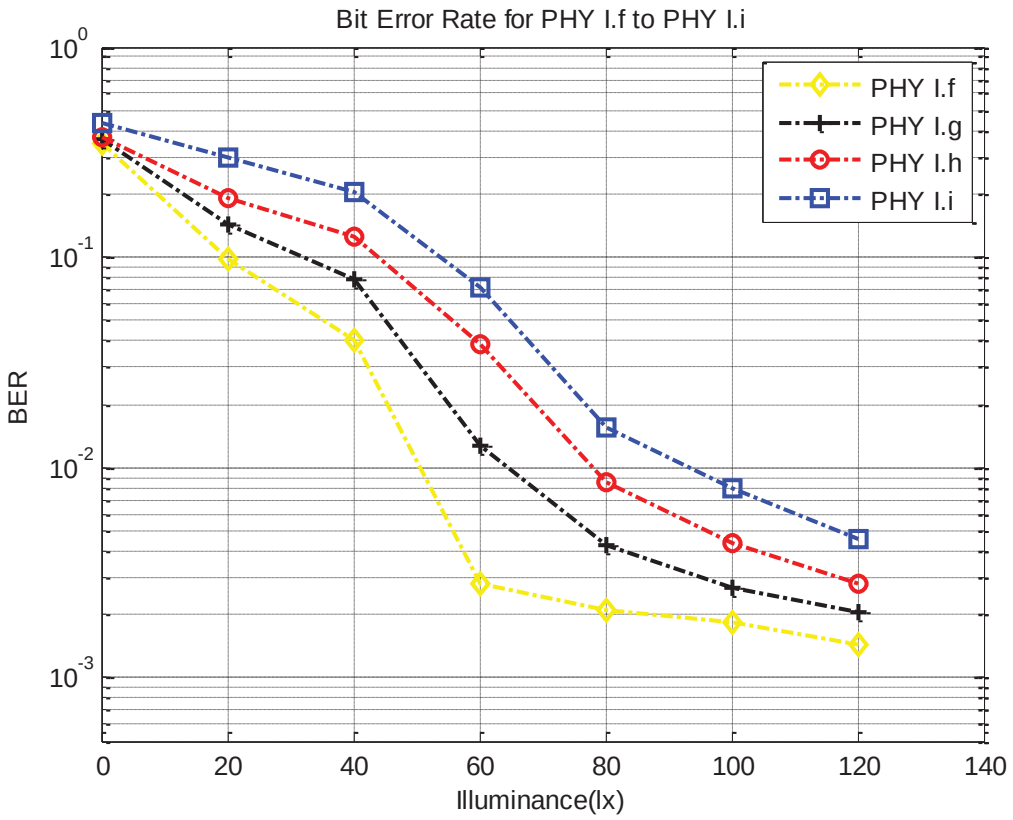

Figure 59: BER VLC HW results of PHY I.f to PHY I.i

4.10 Exp. #10: BER Measurements (MATLAB Simulation AWGN)

In this experiment, we present bit error rate (BER) simulation results of all PHY I modes of IEEE 802.15.7 using MATLAB. Figure 60 provides BER results of modes PHY I.a to PHY I.e, which are based on OOK, and Figure 61 provides BER results of modes PHY I. f to PHY I.g, which use VPPM. The BER is plotted versus SNR.

The actual BER results happen to be different from the simulation results, because, in the simulation environment, we are considering an AWGN channel, whereas, in the real setup, transmission is done inside a room with various light sources present. Furthermore, in order to increase SNR in the real setup, we needed to increase the current from the current source (LED driver) instead of voltage due to

output voltage limitation of USRP. And increasing the current causes the LED to go outside of its linear region.

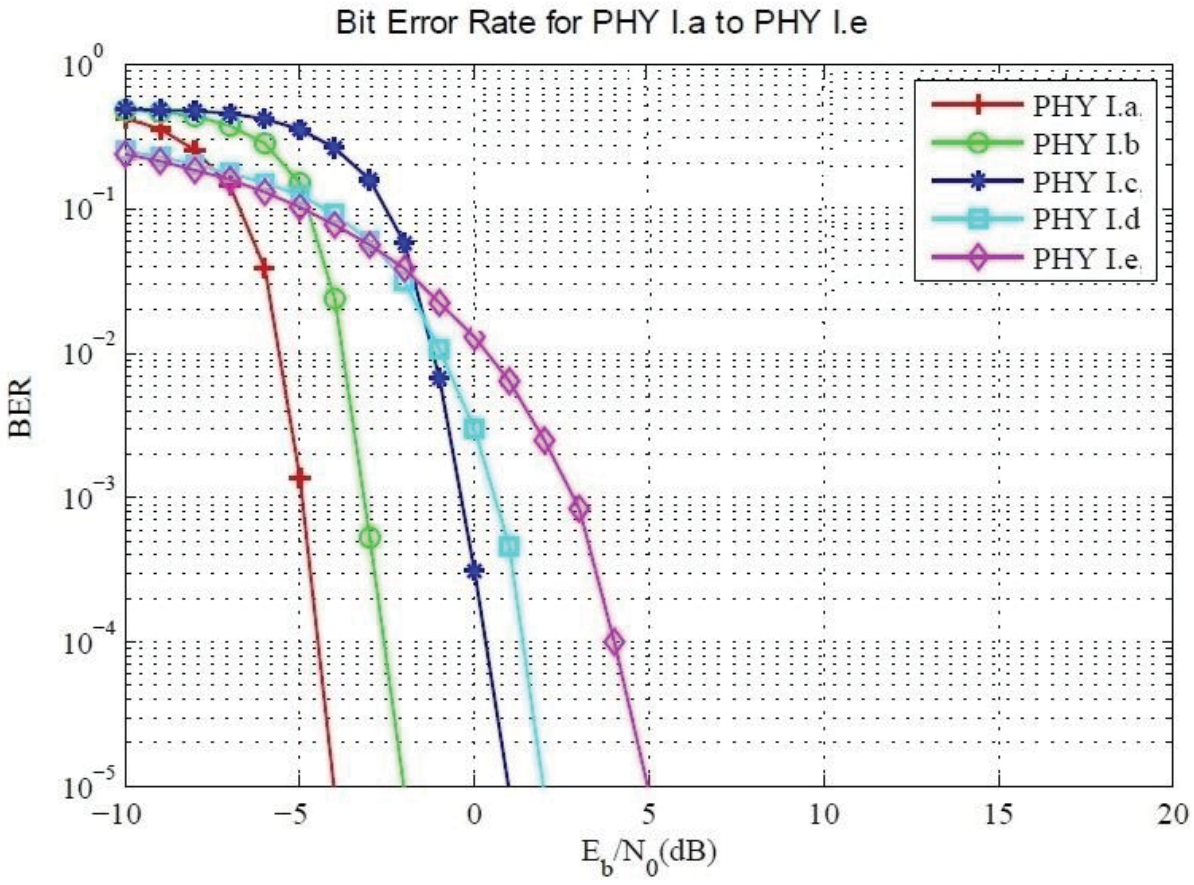

Figure 60: BER AWGN Simulation results of PHY1.a to PHY1.e

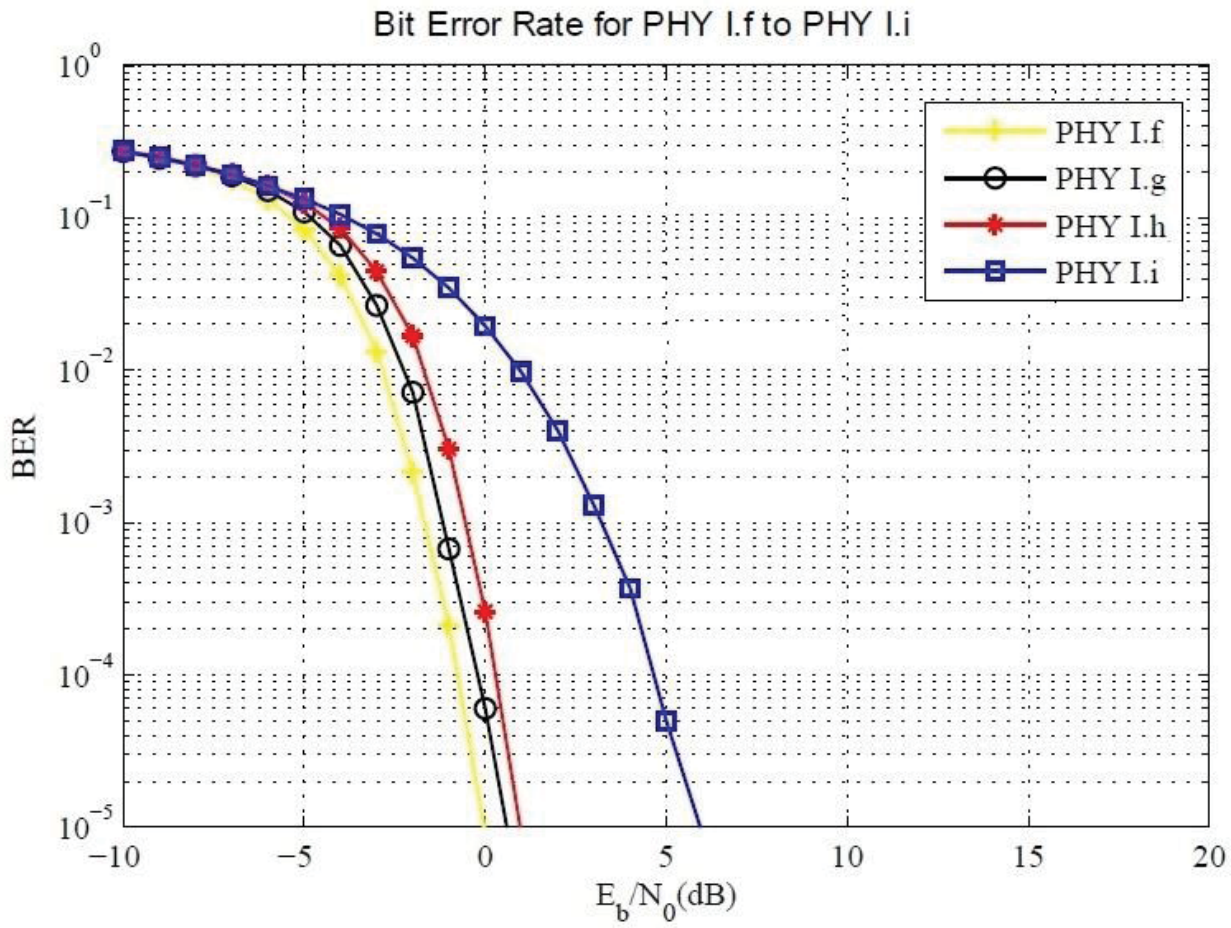

Figure 61: BER AWGN Simulation results of PHY1.f to PHY1.i

4.11 Exp. #11: Audio File Streaming (without bias-tee)

In this experiment, audio streaming is implemented in which any audio file having Microsoft and IBM audio file format compliant WAV audio file is transmitted and successfully received using the above mentioned architecture. With few modifications, our system can support MP3, WMA, and other audio formats.

4.12 Exp. #12: Live Audio Streaming (without bias-tee)

In this experiment, live audio streaming is implemented in which user can speak on the microphone connected to the transmitter, and then audio data is successfully received and recovered on the receiver side. In experiment # 11 and 12, the implementation can support transmission of up to 2 meters.

CHAPTER

V. CONCLUSIONS AND FUTURE WORK

The purpose of this thesis was to implement a fully IEEE 802.15.7 standard-compliant VLC system and carry out performance tests. The VLC literature includes many implementations of higher data rate transmission using various different modulation schemes but standard-compliant implementations are not common place.

This thesis has presented a prototype implementing all 9 PHY I modes of IEEE 802.15.7 standard. The design is based on the widely used SDR platform USRP and visual programming software/language LabVIEW. With the flexibility of SDR platform, other types of PHY algorithms can be easily implemented in LabVIEW and tested through our setup with minimal hardware modification. Furthermore, with our VLC implementation, we successfully demonstrate audio streaming, which can transmit and receive data successfully (@266 kbps) up to 2 meters.

In the future, our VLC design work will be continued by implementing PHY II modes of IEEE 802.15.7 standard. PHY II modes need higher clock frequencies. Furthermore, most advanced versions of SDR based platforms can be used in the future such as NI-PXI with NI LabVIEW Communication Suite.

VLC is a new emerging technology and has many suitable applications. VLC does not seem like it will replace existing Wi-Fi or any other wireless communication systems but it can be used in parallel with those existing systems and will improve the overall user experience.

APPENDIX: EQUIPMENT DETAILS

LED Current Driver:

We used Newport's Laser Diode Driver to drive the LED. It is a pure current source. There are several reasons and advantages for using this current source. First of all, by using this current source we can get the current up to 6 A. This current source has two driving options: (1) driving the load at 3 A (2) driving the load at 6 A. It has a current resolution of 0.03 mA, which provides an opportunity to control the amount of current easily and flexibly. It has an Output-on switch, once we set all the parameters then we can apply current to LED by turning on the Output-on switch. This switch will allow the current flow to the LED approximately after 4 seconds delay. It also has protection circuitry and Error indication LED. Following are the conditions that cause the Error indication LED and its protection circuitry to activate and automatically shutting off the output:

- An open circuit in the LED cabling.
- If the forward voltage drop of the LED exceeds the compliance voltage, which is 5V.
- Over-modulating the external input voltage, to cause the LED output current to exceed the previously set limit value.

After the fault is removed, we turn on the LED by just pressing the Output-on switch.

Figure 62: Laser diode driver (Current source)

Bias tee:

Bias Tee is a 3-port circuit, which is used for setting the DC bias point of electronic equipments without disturbing other equipments. It has 3 ports, namely, (1) DC, (2) RF, and (3) DC+RF. The DC port is the low frequency port used to set the bias point. The RF port passes the radio frequency signal but blocks the DC bias. The RF+DC port provides both RF as well as DC. These 3 ports are sometimes arranged in a "T" shape that's why this device is known as Bias Tee.

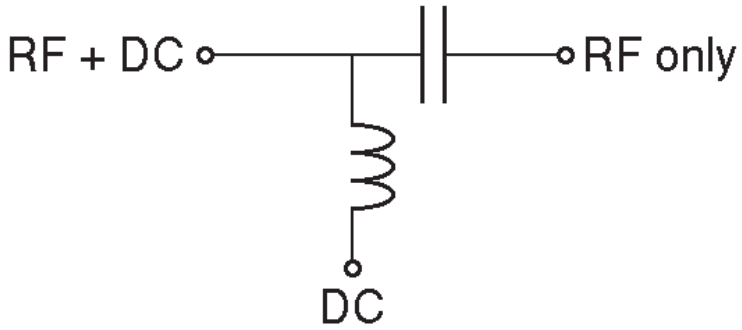

Figure 63: Bias Tee circuit model and connections

Figure 64: Bias-Tee

LED:

The LED used for this thesis is Luminous SST-50 W LED. This LED can give an output of over 1150 lumens just from a single chip. It also has a luminous maintenance of greater than 60 thousand hours. The maximum driving current it can sustain is up to 5 A with a maximum forward voltage of 3.9 V.

Figure 65: LED SST-50

Photodetector:

The photodetector used in our implementation is 'PDA36A-EC' from THORLABS. The 'PDA36A-EC' has reverse-biased Positive Intrinsic Negative (PIN) diode coupled with manual switchable transimpedance amplifier (TIA) gain circuit, ranging from 0 dB to 70 dB. The photodetector has an active area of 3.6 mm x 3.6 mm (13 mm^2) and having a responsivity of 0.1 A/W to 0.5 A/W between visible light range (380 to 780 nm).

Figure 66: Photodetector PDA36A-EC

USRP:

USRP stands for Universal Software Radio Peripheral. It is a software based radio transceiver which is designed actually for wireless communication. USRPs used in this thesis are USRP 2920 having high frequency daughter boards that can be replaced with low frequency daughter boards. By default, USRP 2920 comes with high frequency daughter board, which is WBX 50-2200 MHz Rx/Tx. This daughter board supports high frequency up to 2.2 GHz. On the other hand, we need low frequency daughter board for our VLC application. LFTX and LFRX are the daughter boards, which we are using in this implementation. These daughter boards can support up to 0 Hz to 30 MHz.

Figure 67: USRP 2920

Figure 68: Daughter board WBX 50-2200 MHz Rx/Tx

Figure 69: LFTX daughter board

Figure 70: LFRX daughter board

REFERENCES

[1] M. Kavehrad, "Sustainable Energy-Efficient Wireless Applications Using Light," IEEE Communications Magazine, Dec. 2010.

[2] R.D. Dupuis and M.R. Krames, "History, Development, and Applications of High-Brightness Visible Light-Emitting Diodes," IEEE J. Lightwave Tech., vol. 26, no. 9, pp. 1154-1170, 2008.

[3] "Phasing out incandescent bulbs in the EU-Technical briefing," available at http://ec.europa.eu/energy/efficiency/ecodesign/doc/committee/2008_12_08_technical_briefing_household_lamps.pdf

[4] "Member States approve the phasing–out of incandescent bulbs by 2012," EU Press Release, 8 Dec. 2008.

[5] S. Arnon, J.R. Barry, G.K. Karagiannidis, R. Schober, and M. Uysal (Eds.), Advanced Optical Wireless Communication, Cambridge University Press, Jul. 2012.

[6] T. Komine and M. Nakagawa, "Fundamental analysis for visible-light communication system using LED lights," IEEE Transactions on Consumer Electronics, vol. 50, no. 1, pp. 100-107, 2004.

[7] G. Ntogari, T. Kamalakis, J. Walewski, and T. Sphicopoulos, "Combining illumination dimming based on pulse-width modulation with visible light communications based on discrete multitone," Journal of Optical Communications and Networking, vol. 3, no. 1, pp. 56-65, 2011.

[8] S. Arnon, J. Barry, G. Karagiannidis, R. Schober, and M. Uysal (Eds.), Advanced optical wireless communication systems. Cambridge University Press, 1st ed., 2012.

[9] D. O'Brien and et al., "Indoor visible light communications: challenges and prospects," in Proc. of SPIE, vol. 7091, 2008.

[10] M. Kavehrad, "Broadband Room Service by Light," Scientific American, pp. 82-87, Jul. 2007.

[11] Z. Ghassemlooy, W. Popoola, and S. Rajbhandari, Optical wireless communications: system and channel modelling with MATLAB. 1st ed., 2012.

[12] Japan Electronics and Information Technology Industries Association (JEITA), "Visible Light Communication CP-1221, CP-1222 specifications," Japan, 2007.

[13] IEEE Standard, "802.15.7: IEEE standard for local and metropolitan area networks. Part 15.7: Short Range Wireless Optical Communication using Visible Light," Sep. 2011.

[14] M. Noshad and M. Brandt-Pearce, "Can visible light communications provide Gb/s service?" IEEE Communications Magazine, 2013.

[15] Z. Ghassemlooy, W. Popoola, and S. Rajbhandari, Optical Wireless Communications - System and Channel Modelling with MATLAB, CRC publisher, USA, August 2012, ISBN: 978-4398-5188-3.

[16] K. Asadzadeh, Efficient OFDM Signaling Schemes for Visible Light Communication Systems. M.Sc. Thesis, Hamilton, Canada, 2011.

[17] T.L. Floyd, Electronic Devices: Conventional Current Version, 9th Ed., Prentice Hall, USA, 2012, ISBN-13: 978-0-13-254986-8, ISBN-10: 0-13-254986-7.

[18] K. Kishino, M.S. Unlu, J.I. Chyi, J. Reed, L. Arsenault, and H. Morkoc, "Resonant cavity-enhanced (RCE) photodetectors," IEEE Journal of Quantum Electronics, 27, pp. 2025-2034, 1991.

[19] Y.-G. Wey, K.S. Giboney, J.E. Bowers, M.J.W. Rodwell, P. Silvestre, P. Thiagarajan, and G.Y. Robinson, "108 GHz GaInAs/InP p-i-n photodiodes with integrated bias tees and matched resistors," IEEE Photonics Technology Letters, vol. 5, pp. 1310-1312, 1993.

[20] K. Kato, "Ultrawide-band/high-frequency photodetectors," IEEE Transactions on Microwave Theory and Techniques, 47, 1265-1281, 1999.

[21] K. Shiba, T. Nakata, T. Takeuchi, T. Sasaki, and K. Makita, "10 Gbit/s asymmetric waveguide APD with high sensitivity of -30 dBm," Electronics Letters, vol. 42, pp. 1177-1178, 2006.

[22] A. Jovicic, J. Li, and T. Richardson, "Visible light communication: Opportunities, challenges and the path to market," IEEE Communications Magazine, vol. 51, no. 12, pp. 26-32, 2013.

[23] L. Grobe, A. Paraskevopoulos, J. Hilt, D. Schulz, F. Lassak, F. Hartlieb, C. Kottke, V. Jungnickel, and K.-D. Langer, "High-speed visible light communication systems," IEEE Communications Magazine, vol. 51, no. 12, pp. 60-66, 2013.

[24] P.A. Haigh, T.T. Son, E. Bentley, Z. Ghassemlooy, H. Le Minh, and L. Chao, "Development of a Visible Light Communications System for Optical Wireless Local Area Networks," in Proc. IEEE Computing, Communications and Applications Conference (ComComAp), pp. 351-355, Hong Kong, China, Jan. 2012.

[25] C. Kottke et al., "1.25Gbit/s Visible Light WDM Link based on DMT Modulation of a Single RGB LED Luminary," European Conference and Exhibition on Optical Communications (ECOC), pp. 1-3, Amsterdam, Netherlands, Sep. 2012.

[26] H. Elgala, R. Mesleh, and H. Haas, "Indoor broadcasting via white LEDs and OFDM," IEEE Trans. Consumer Electron., vol. 55, no. 3, pp. 1127-1134, 2009.

[27] M.Z. Afgani, H. Haas, H. Elgala, and D. Knipp, "Visible Light Communication Using OFDM," in Proc. Of International Conference on Testbeds and Research Infrastructures for the Development of Networks and Communities (TRIDENTCOM), pp. 129-134, Barcelona, Spain, Mar. 2006.

[28] O. Bouchet, P. Porcon, M. Wolf, L. Grobe, J.W. Walewski, S. Nerreter, K. Langer, L. Fernandez, J. Vucic, T. Kamalakis, G. Ntogari, and E. Gueutier, "Visible-light communication system enabling 73Mb/s data streaming," in Proc. IEEE Globecom Workshop on Optical Wireless Communications, pp. 1042-1046, Miami, USA, Dec. 2010.

[29] M. Guerra-Medina, B. Rojas-Guillama, O. Gonzalez, J. Martin-Gonzalez, E. Poves, and F. Lopez-Hernandez, "Experimental optical code-division multiple access system for visible light communications," in Proc. Wireless Telecommunications Symp., New York, USA, pp. 1-6, 2011.

[30] H. Elgala, R. Mesleh, H. Haas, and B. Pricope, "OFDM Visible Light Wireless Communication Based on White LEDs," in Proc. of IEEE Vehicular Technology Conference (VTC), pp. 2185-2189, Dublin, Ireland, Apr. 2007.

[31] Y. Qiao, H. Haas, and E. Knightly, "A Software-defined Visible Light Communications System with WARP," 1st ACM MobiCom Workshop on VLC Systems, Sep. 2014.

[32] M. Rahaim, T. Borogovac, T.D.C. Little, A. Mirvakili, and V. Joyner, “Demonstration of a Software Defined Visible Light Communication System,” in Demo and Exhibits of International Conference on Mobile Computing and Networking, Las Vegas, USA, Sep. 2011.

[33] J. Baranda, P. Henarejos, and C. Gavrincea, “An SDR Implementation of a Visible Light Communication System based on IEEE 802.15.7 Standard,” in Proc. International Conference on Telecommunications, pp. 1-5, Casablanca, Morocco, May 2013.

[34] R. Farrell, M. Sanchez, and G. Corley, “Software-Defined Radio Demonstrators: An Example and Future Trends,” International Journal of Digital Multimedia Broadcasting, vol. 2009, Article ID 547650, 12 pages, 2009.

[35] “Wireless Open Access Research Platform (WARP)" [Online]. Available at: http://warpproject.org

[36] “GNU Radio, the GNU Software Radio project” [Online]. Available at: http://gnuradio.org/redmine/projects/gnuradio/wiki

[37] “Ettus Research” [Online]. Available at: http://www.ettus.com

[38] “Flexible Communications (FlexiCom)” [Online]. Available at: http://flexicom.redyc.com

[39] S. Rajagopal, R.D. Roberts, and S.K. Lim, “IEEE 802.15.7 visible light communication: Modulation schemes and dimming support,” IEEE Communications Magazine, vol. 50, no. 3, pp. 72-82, Mar. 2012.

[40] R.D. Roberts, S. Rajagopal, and S.K. Lim, “IEEE 802.15.7 physical layer summary,” in IEEE Globecom Workshops (GC Wkshps), pp. 772-776, 2011.

[41] S. Berman et al., “Human Electroretinogram Responses to Video Displays, Fluorescent Lighting and Other High Frequency Sources,” Optometry and Vision Science, vol. 68, pp. 645-662, 1991.

[42] W.A. Geisel, “Tutorial on Reed-Solomon Error Correction Coding,” National Aeronautics and Space Administration (NASA) Tech. Briefs, Lyndon B. Johnson Space Center, Houston, Texas, 1990.

[43] E. Sarbazi and M. Uysal, “PHY layer performance evaluation of the IEEE 802.15.7 visible light communication standard,” in. Proc. of Int. Workshop Opt. Wireless Communications, Oct. 2013.

[44] W. Husain, H. F. Ugurdag and M. Uysal, “Software defined VLC System: Implementation and Performance Evaluation,” in. Proc. of Int. Workshop Opt. Wireless Communications, Istanbul, Sep. 2015.